LIPEI DU

DEPARTMENT OF PHYSICS, MCGILL UNIVERSITY

EXPLORING INITIAL AND FINAL BARYON DISTRIBUTIONS IN HEAVY-ION COLLISIONS AT BEAM ENERGY SCAN

L. Du, C. Shen, S. Jeon & C. Gale, arXiv:2211.16408； L. Du, H. Gao, S. Jeon & C. Gale, arXiv:2302.13852

THE MANY FACES OF RELATIVISTIC FLUID DYNAMICS

UC SANTA BARBARA, KAVLI INSTITUTE FOR THEORETICAL PHYSICS

JULY 11, 2023

BACKGROUND & MOTIVATION

QCD PHASE DIAGRAM

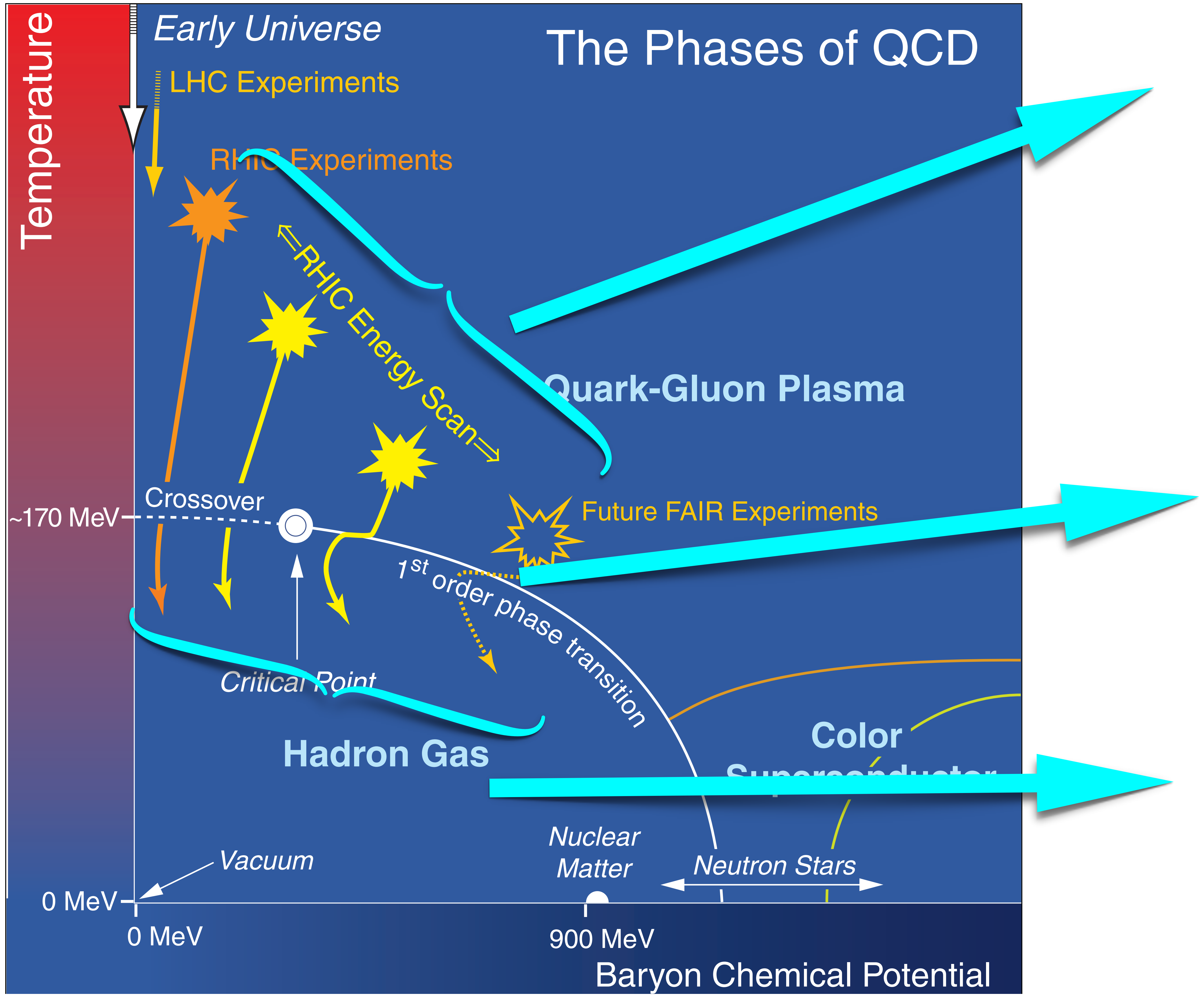

2007 NSAC Long Range Plan

- Starting: initial baryon distribution
- Trajectory: hydrodynamics
- End: final baryon distribution

RAPIDITY-DEPENDENT MEASUREMENTS

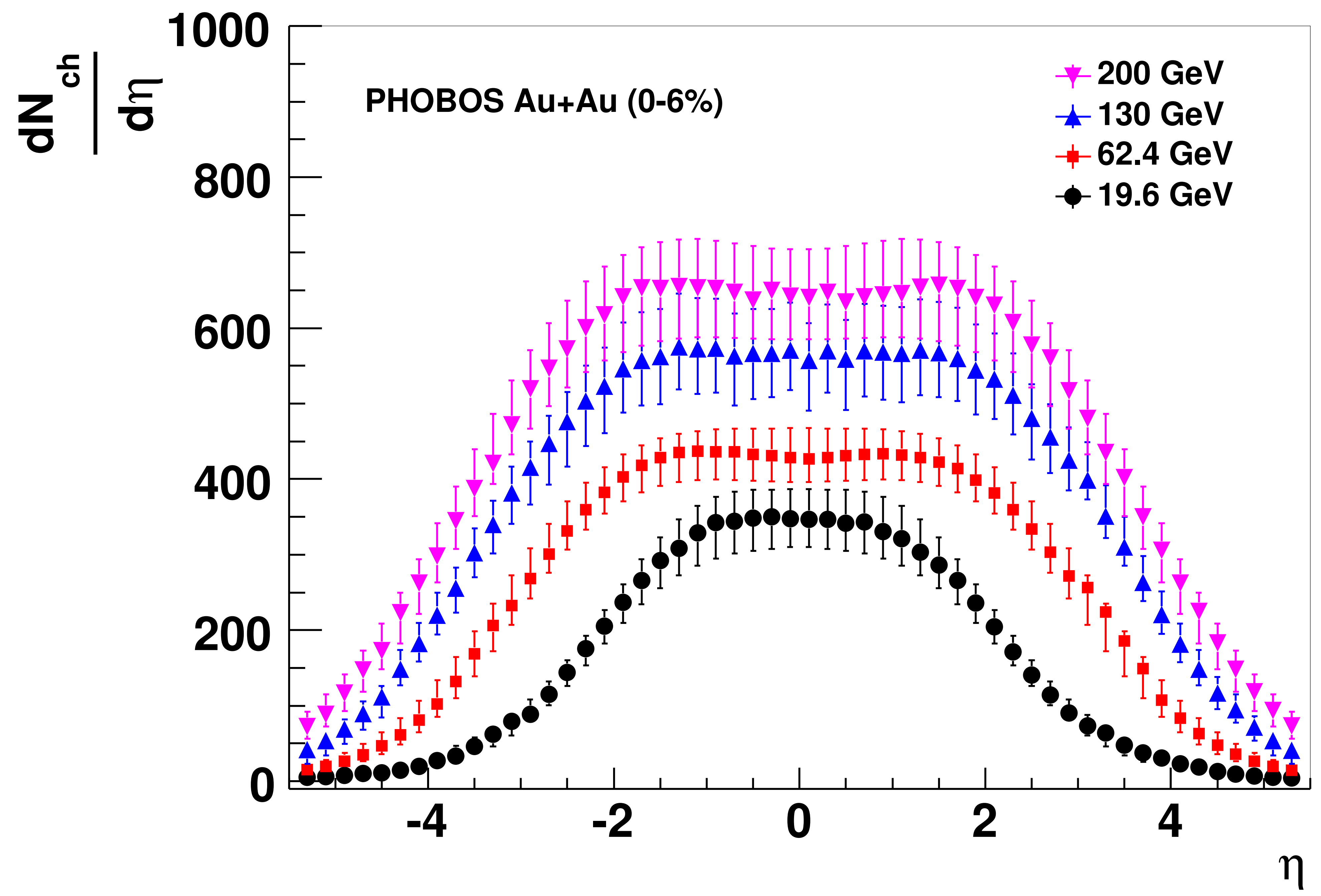

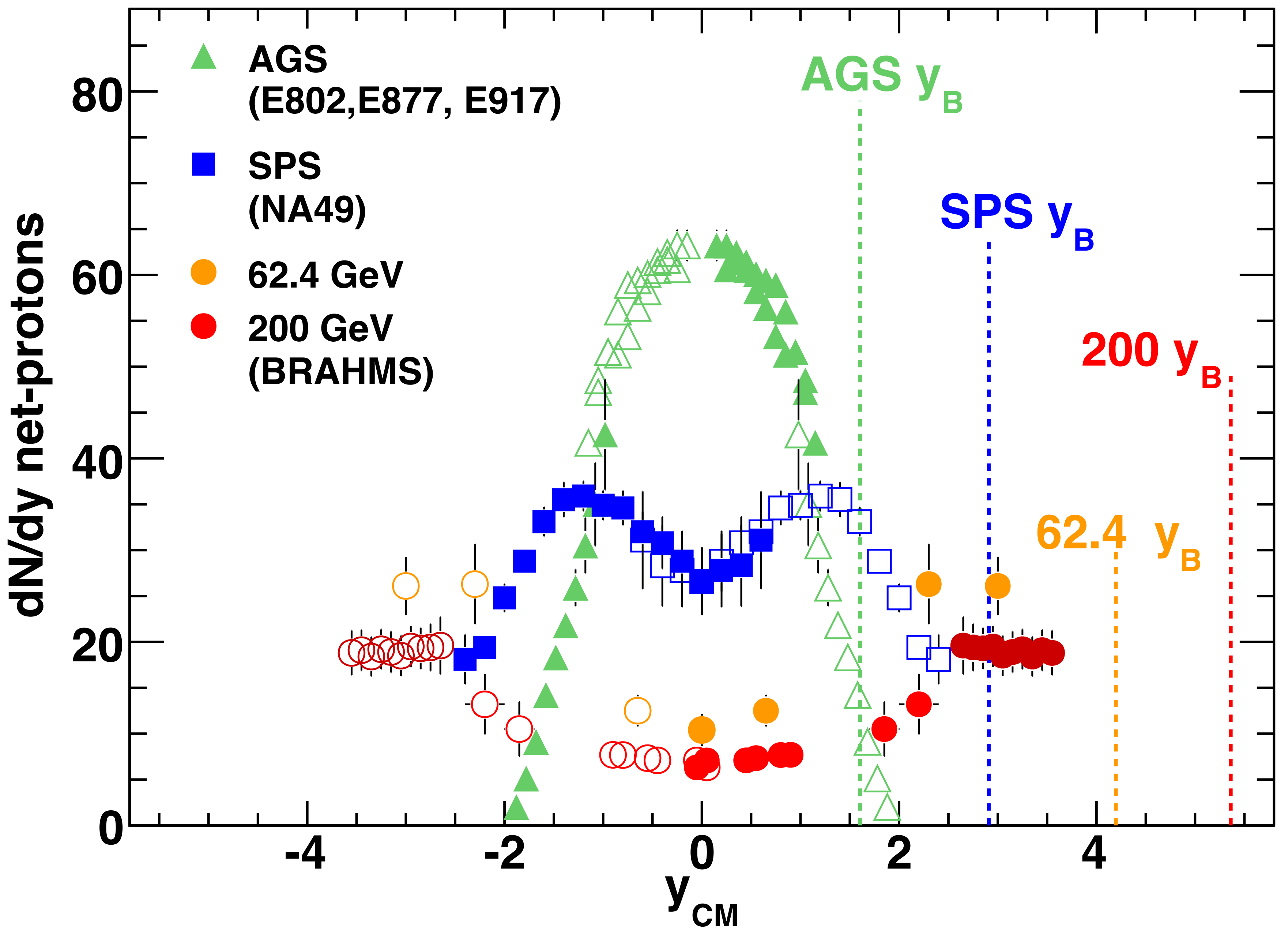

Pseudo-rapidity (rapidity) distribution of charged particles (net protons) at different collision energies

- Rapidity-dependent measurements are essential for constraining theoretical models:
  - Charged particle multiplicity → entropy/energy density
  - Net-proton distribution → baryon density

Figs refs: R. Sahoo et al., 1408.5773; F. Videbaek, Nucl. Phys. A 830 (2009) 43C

LONGITUDINAL DYNAMICS & BARYON EVOLUTION

- Dynamics at Beam Energy Scan:
  - Longitudinal dynamics
  - Baryon charge evolution
- Rapidity scan:
  - Each rapidity window probes a different part of the phase diagram
  - More opportunities for finding critical phenomena.

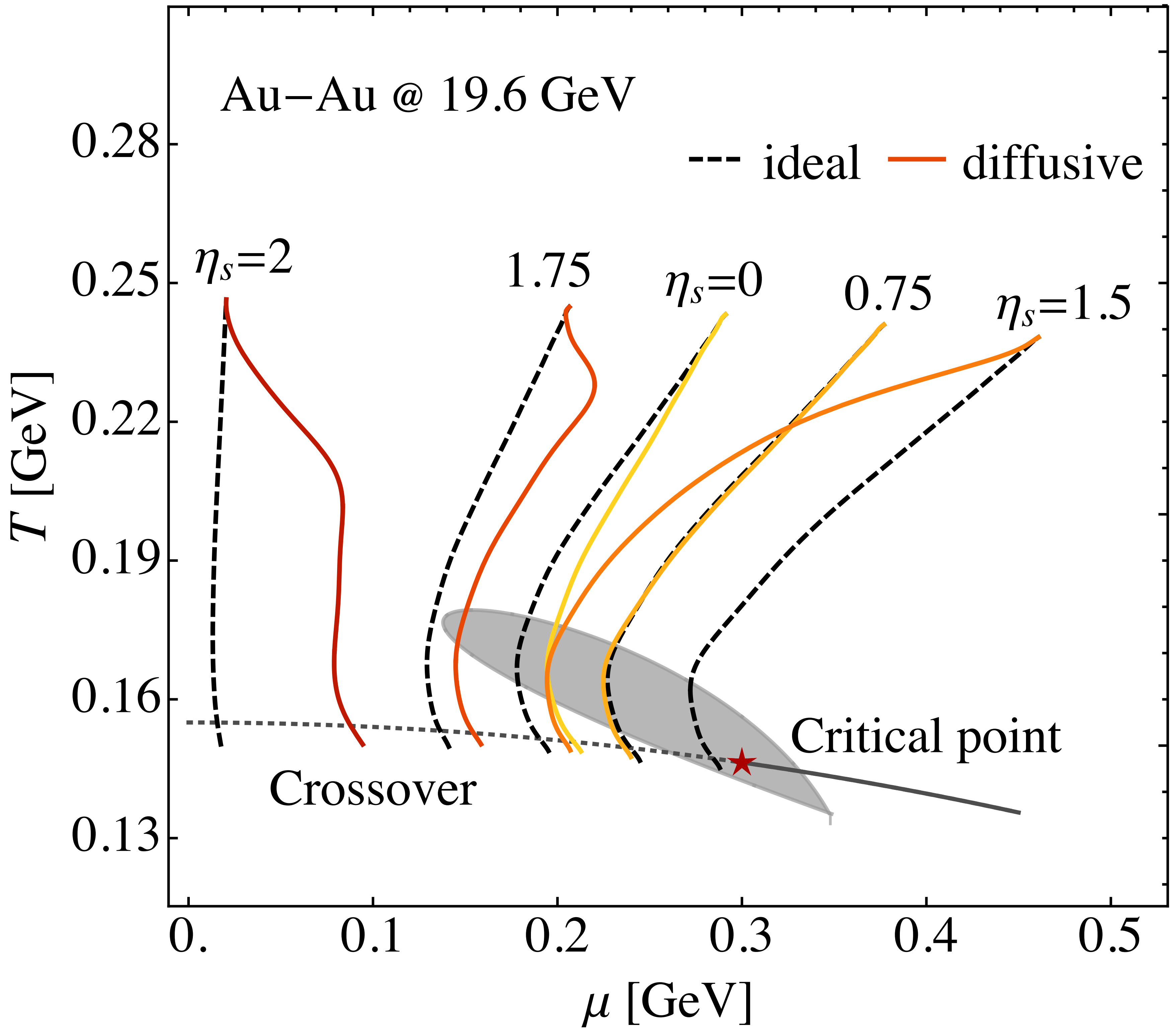

LD, X. An and U. Heinz, PRC 104, 064904 (2021); CPOD21, 2109.06918

MULTI-STAGE EVOLUTION

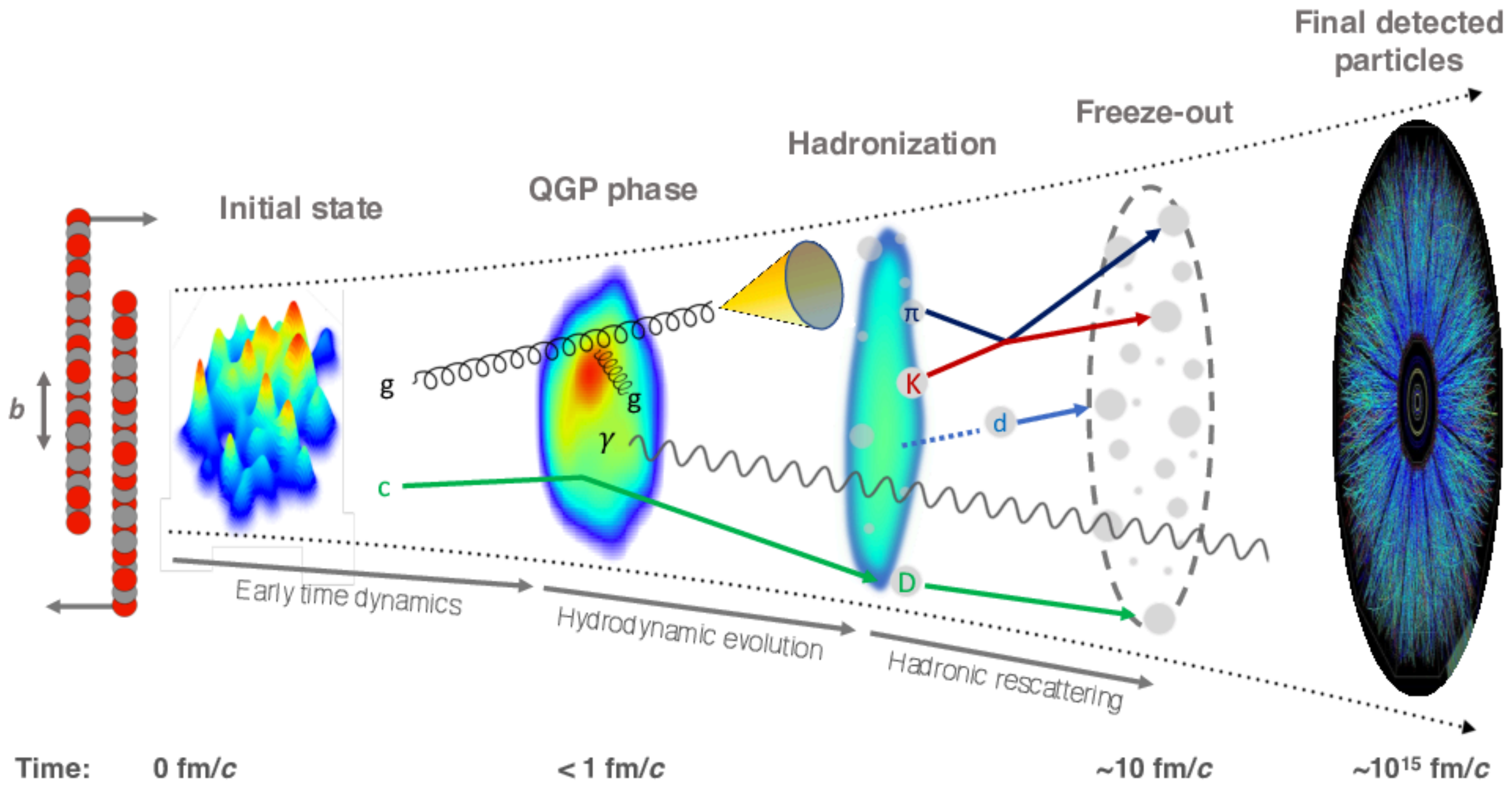

Fig ref: Hot QCD White Paper, M. Arslandok, et al., arXiv: 2303.17254

MULTI-STAGE HYDRODYNAMIC MODEL

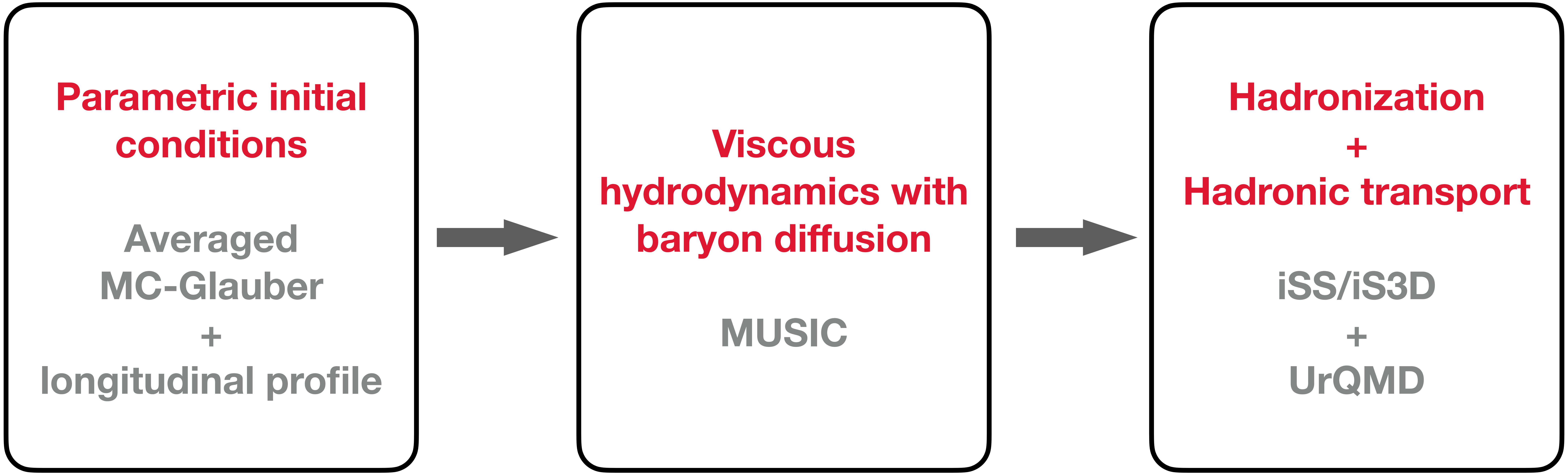

Denicol et al, PRC 98, 034916 (2018); Shen and Alzhrani, PRC102, 014909 (2020); LD, C. Shen, S. Jeon & C. Gale, arXiv:2211.16408; LD, H. Gao, S. Jeon & C. Gale, arXiv:2302.13852

CALIBRATION OF THE MODEL

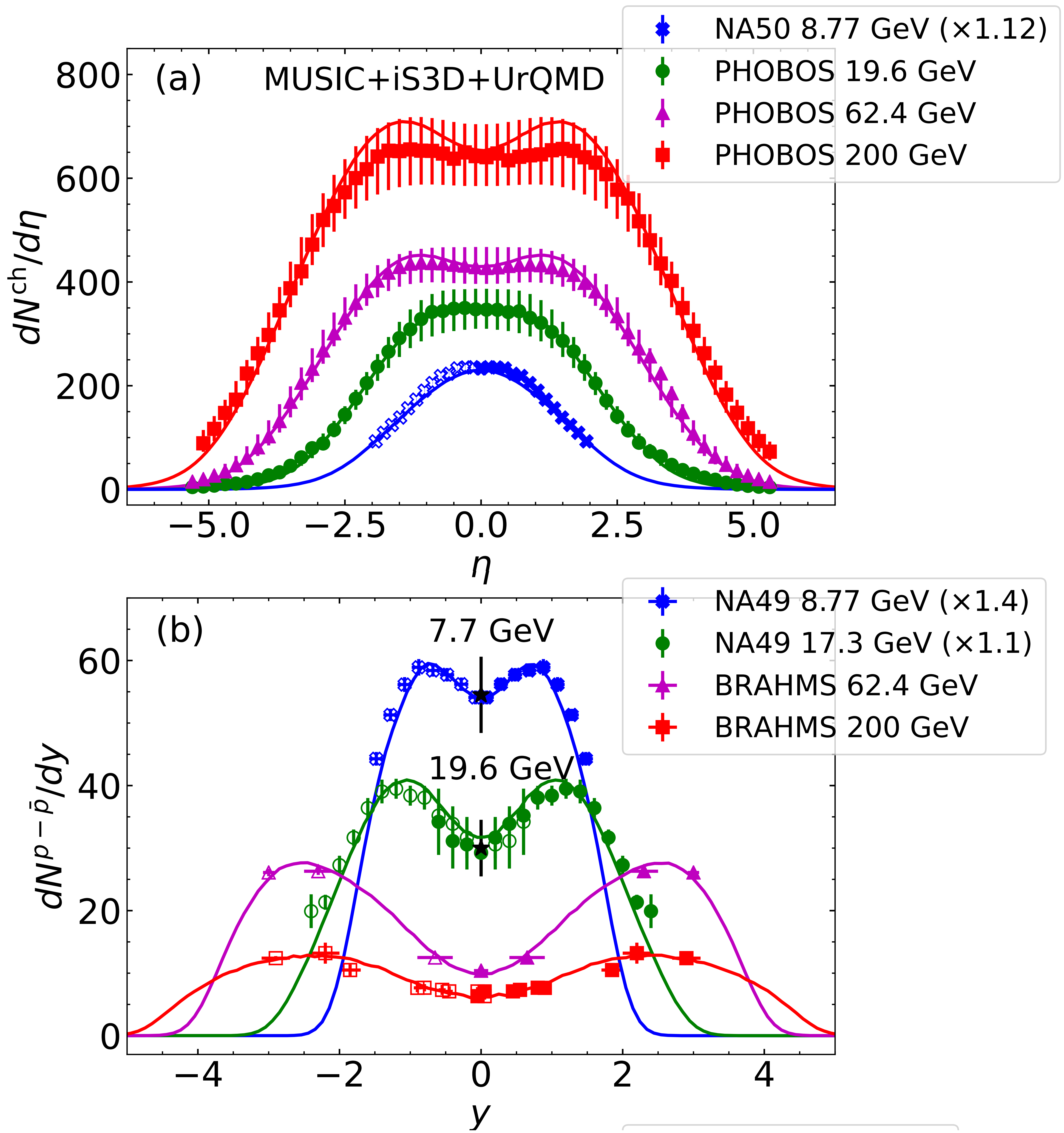

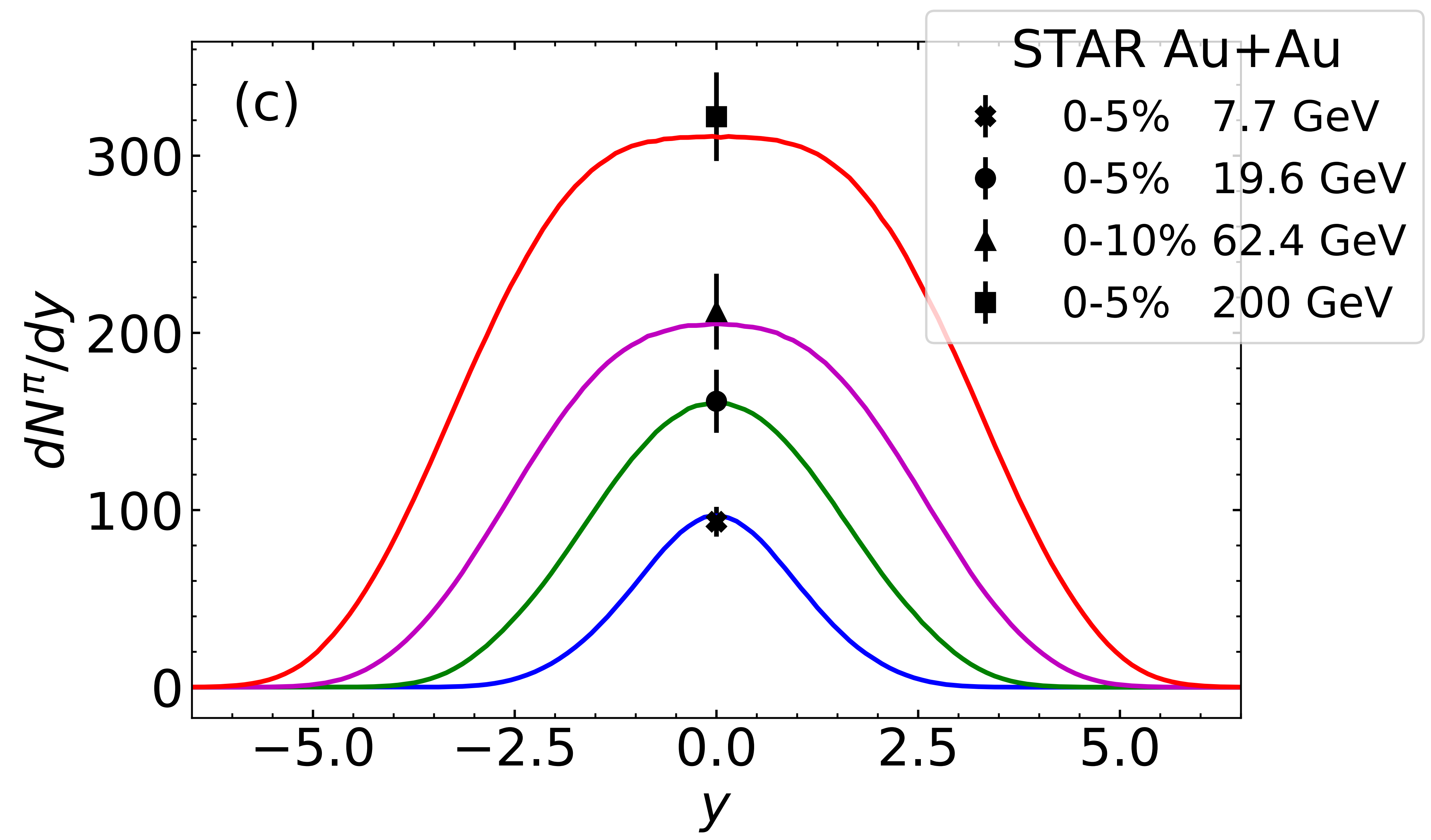

- Calibrate central Au+Au collisions at $\sqrt{s_{\mathrm{NN}}} = 7.7, 19.6, 62.4, 200$ GeV
- Au+Au @ 7.7 GeV: rescaled data from Pb+Pb @ 8.7 GeV
- Au+Au @ 19.6 GeV: rescaled data from Pb+Pb @ 17.3 GeV

PROBING INITIAL BARYON DISTRIBUTION

DIRECTED FLOW OF IDENTIFIED PARTICLES

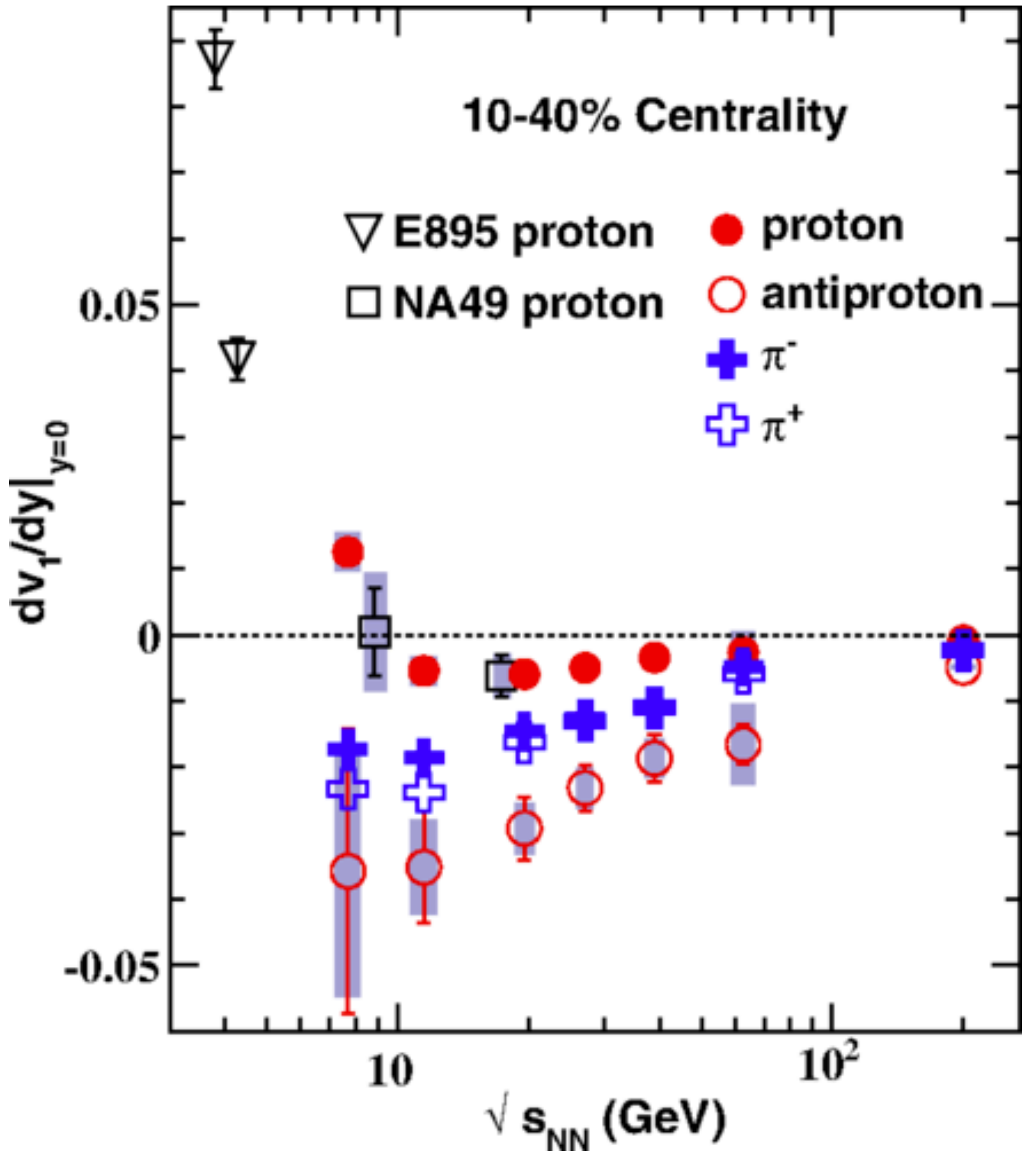

Data: STAR, PRL 112, 162301 (2014)

STAR, PRL 120, 062301 (2018)

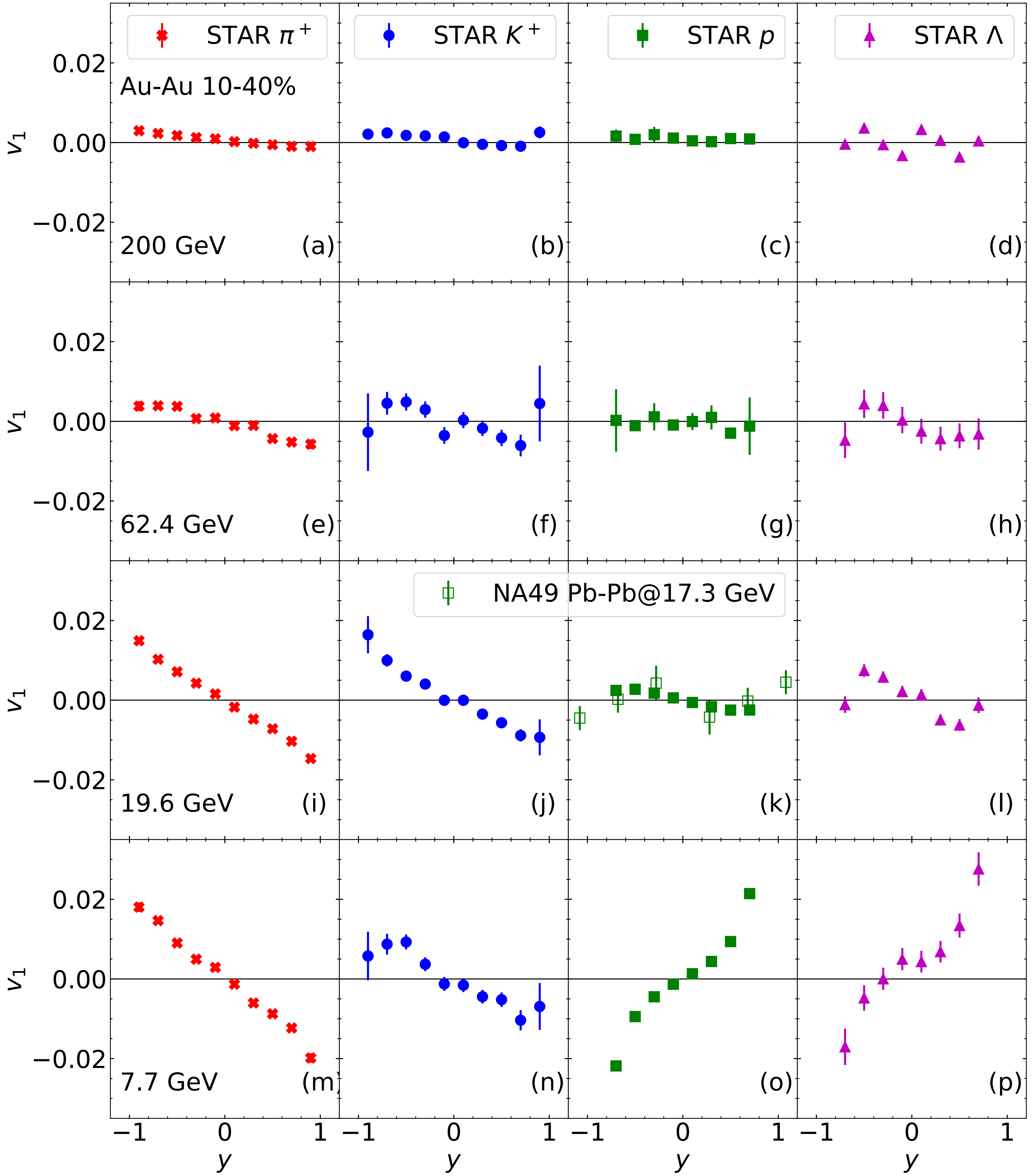

- Directed flow $v_1(y)$: collective sideward motion of final particles;
- Measurements from STAR and NA49 for intermediate-centrality collisions show various beam energy dependence for $v_1(y)$ of identified particles– challenging to explain.

BARYON STOPPING & $v_1(y)$ OF BARYONS

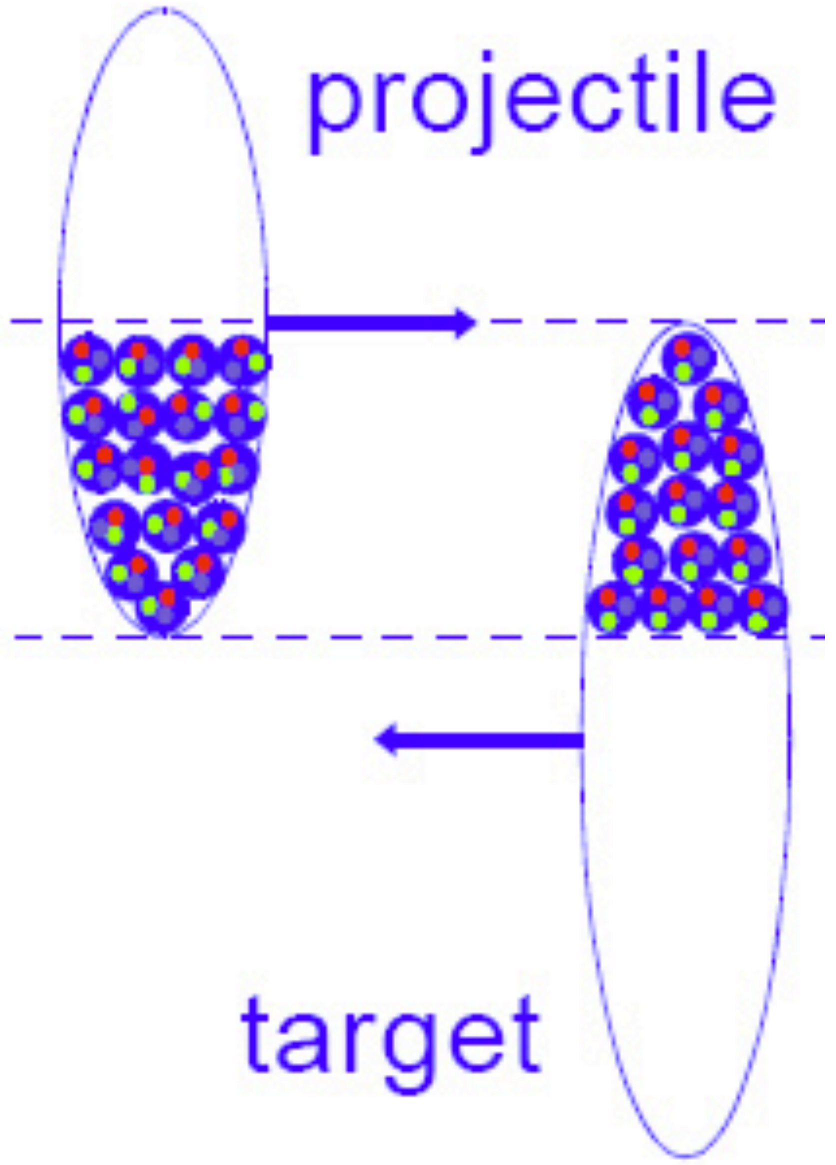

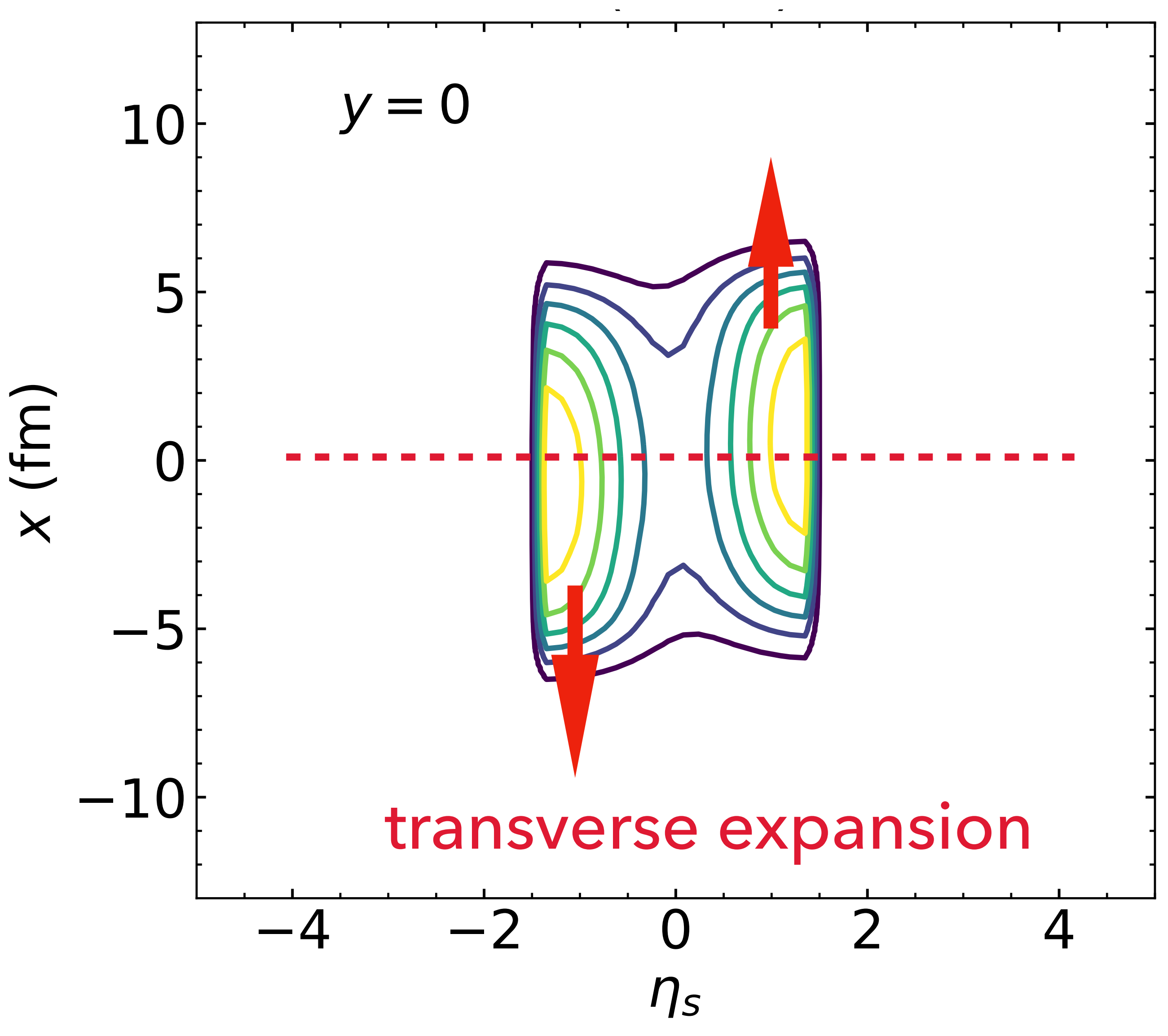

initial baryon distribution

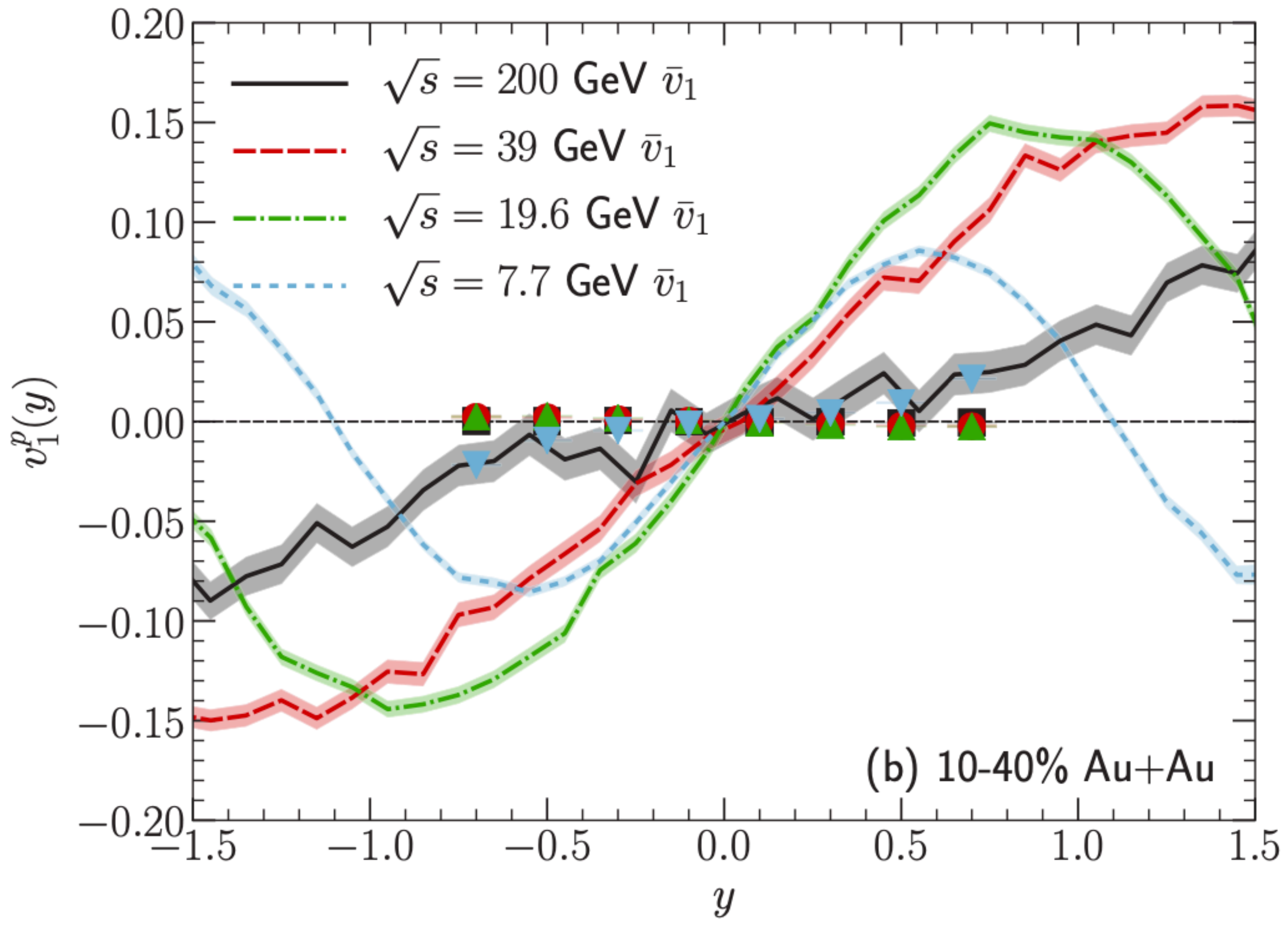

Shen and Alzhrani, PRC102, 014909 (2020)

- The widely used baryon stopping picture results in $v_1(y)$ strongly overshooting the experimental measurements for protons at all beam energies;
- $v_1(y)$ of baryons is mainly driven by asymmetric distribution of baryon density with respect to beam axis + transverse expansion.

$dN^{p-\bar{p}}/dy$ AND $v_1(y)$ OF PROTONS

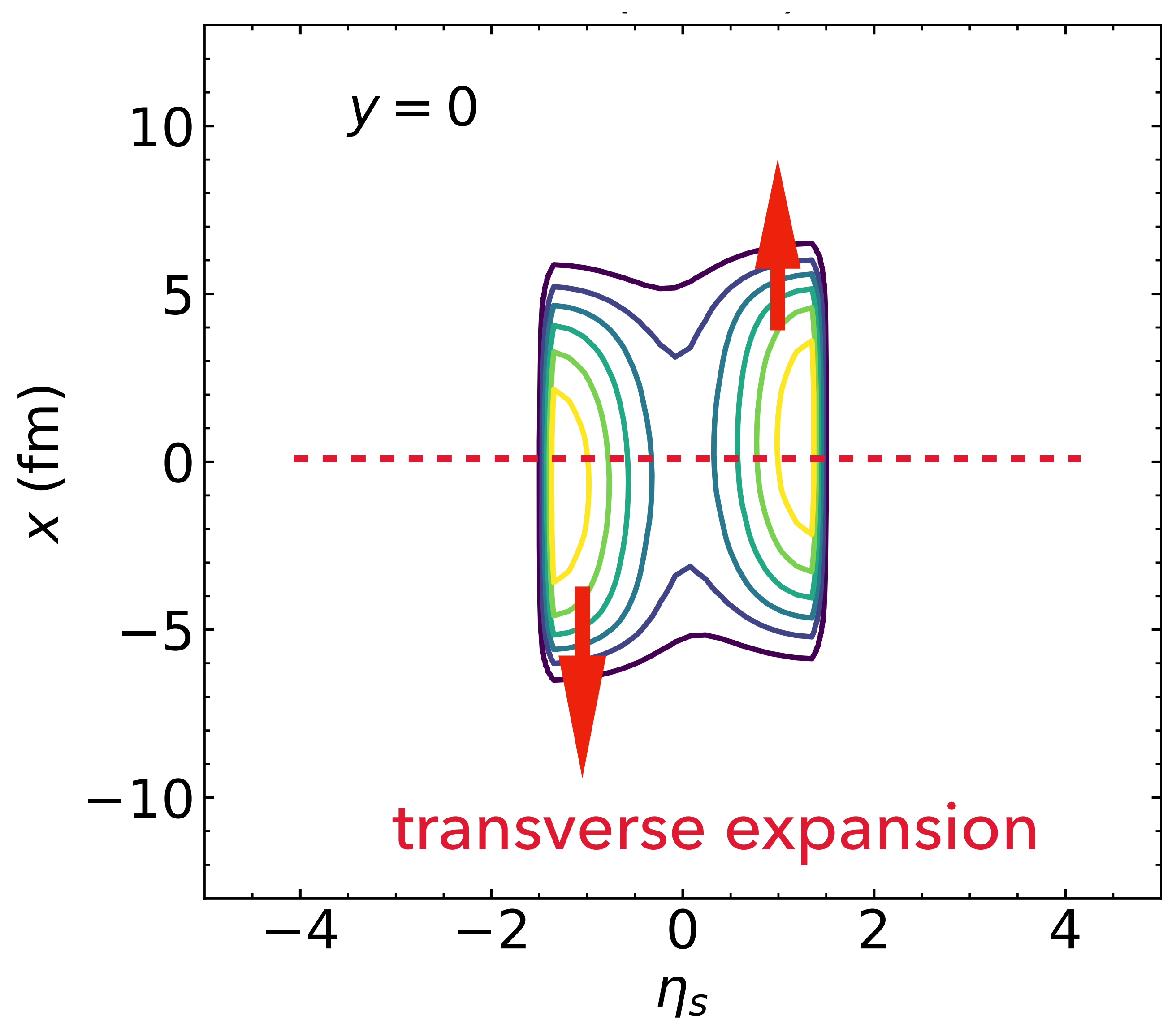

initial baryon distribution

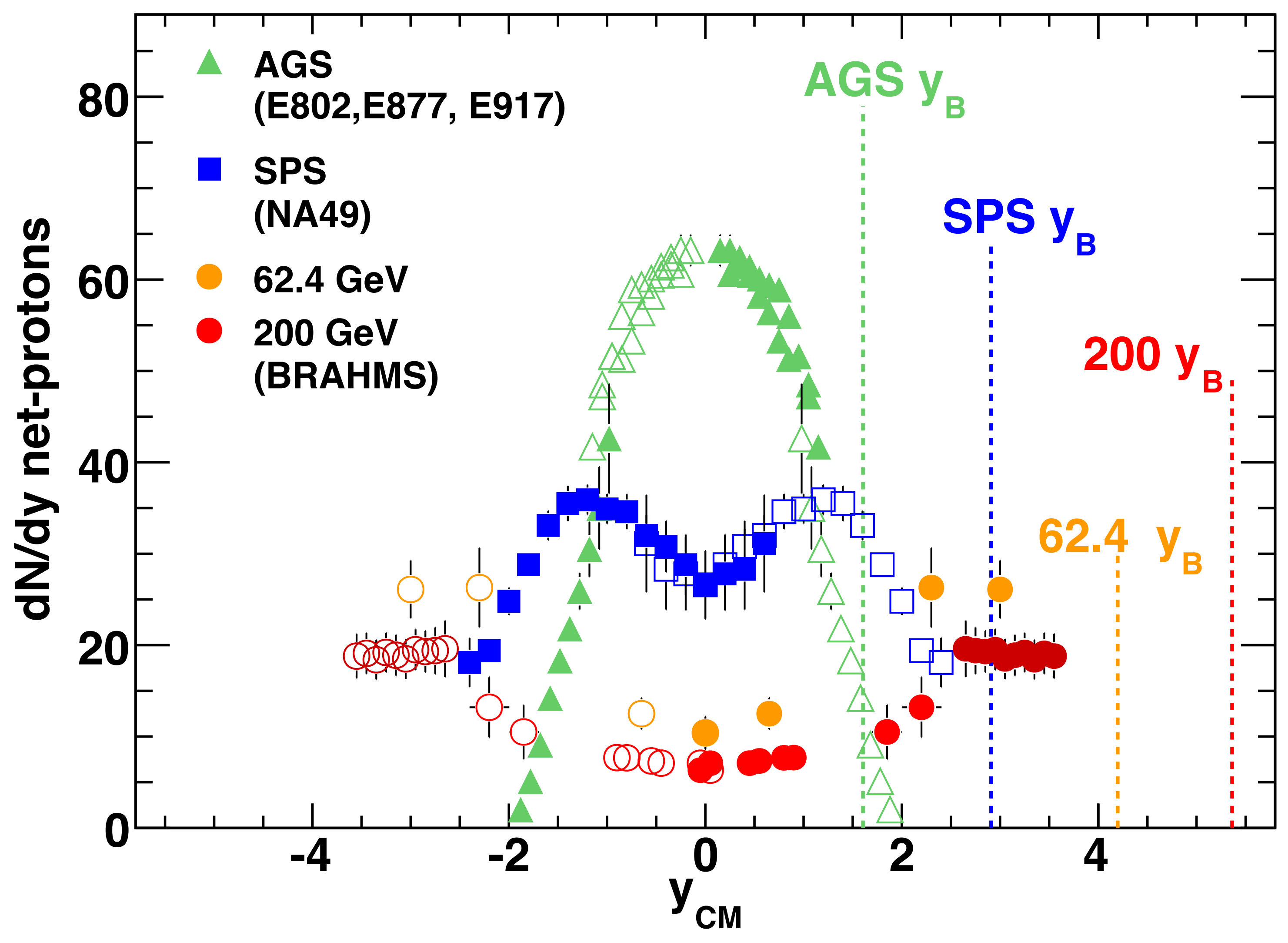

F. Videbaek, Nucl. Phys. A 830 (2009) 43C

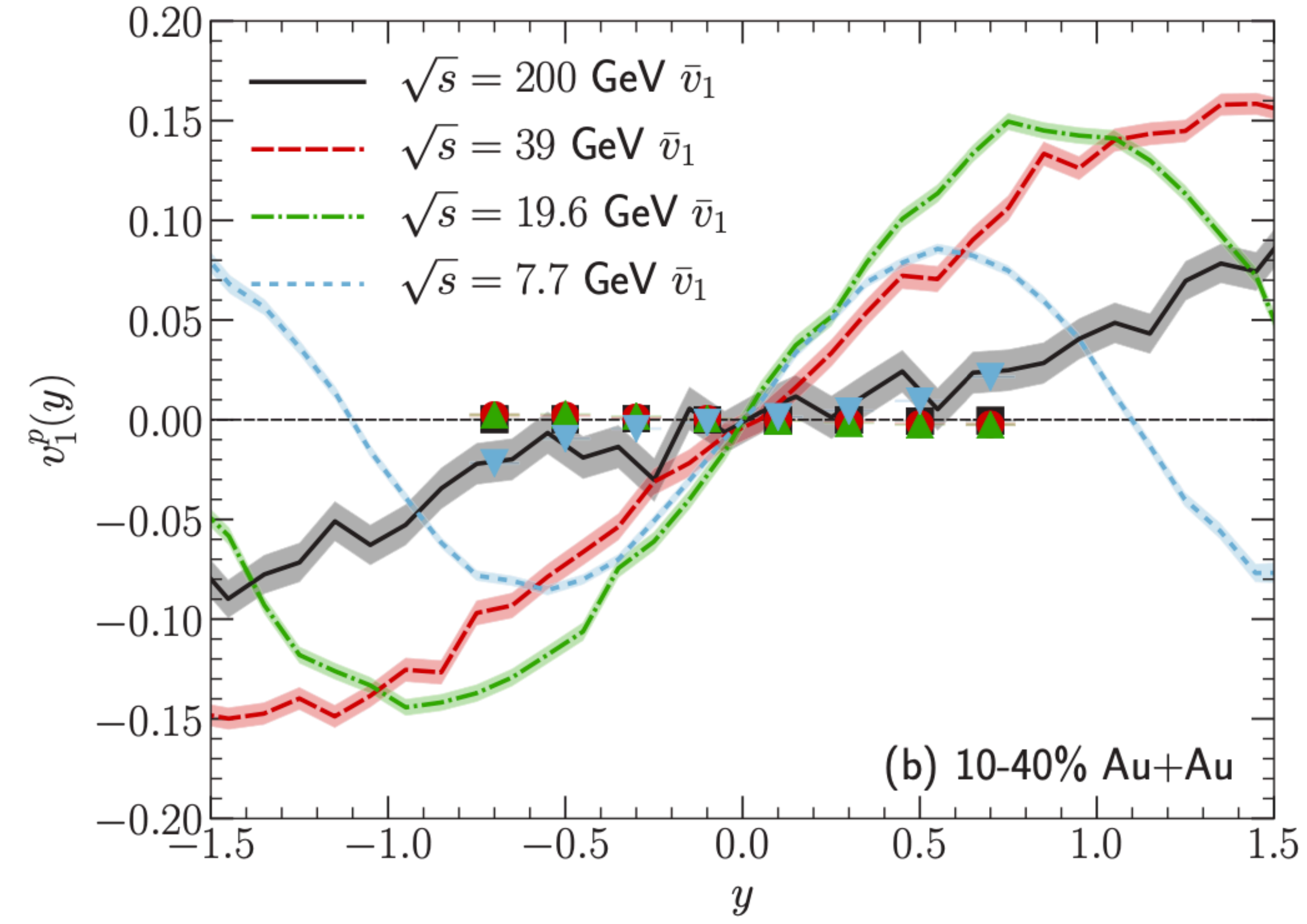

Shen and Alzhrani, PRC102, 014909 (2020)

- Reducing baryon density around midrapidity can reduce $v_1(y)$, but not enough net protons can be achieved.
- Challenge: explaining the rapidity distributions of net proton yield and proton directed flow simultaneously
  - Rapidity distribution of net protons: double-humped structure
  - Directed flow of protons: extremely small compared to theoretical calculations

PARAMETRIC INITIAL CONDITIONS

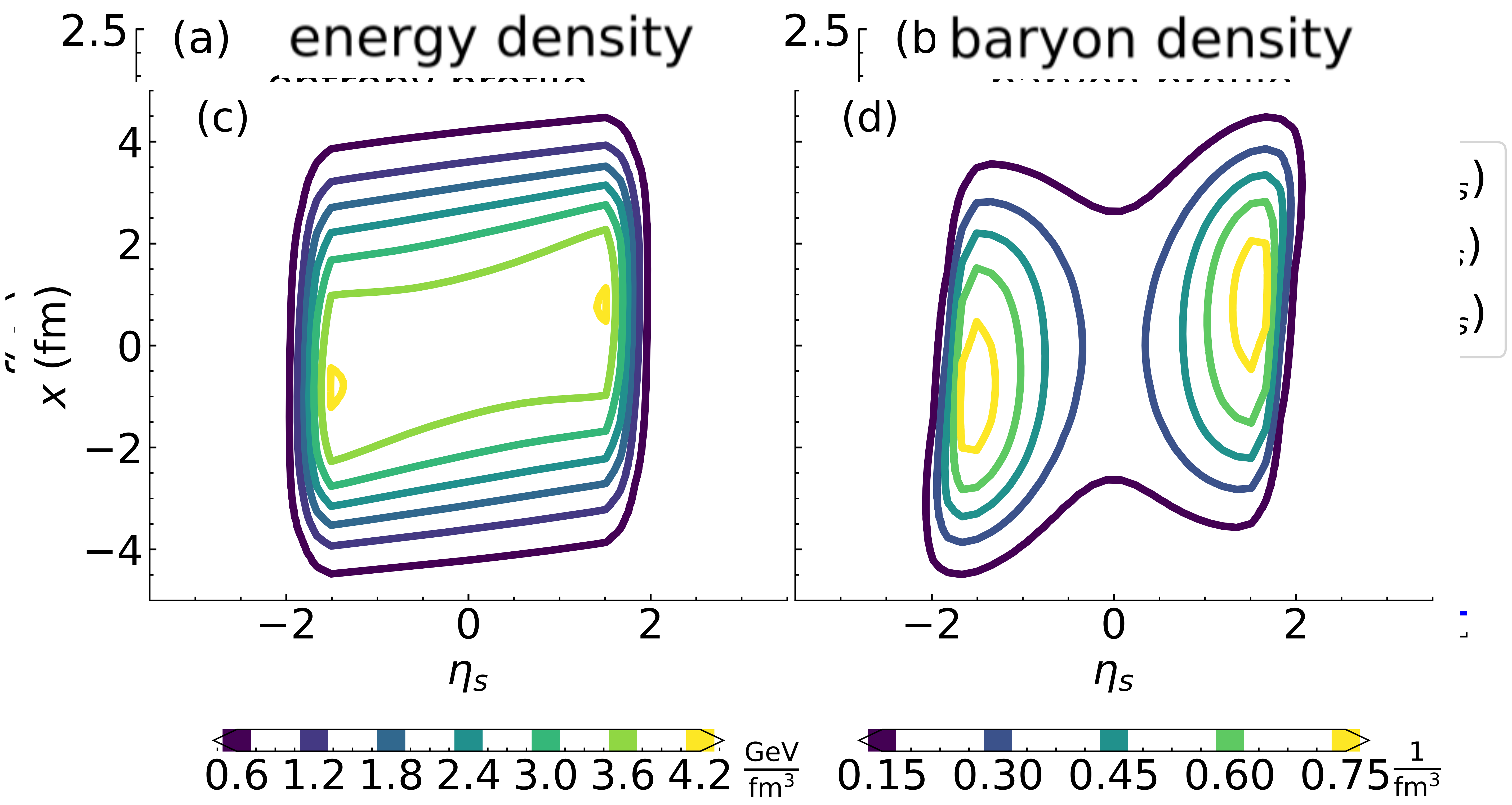

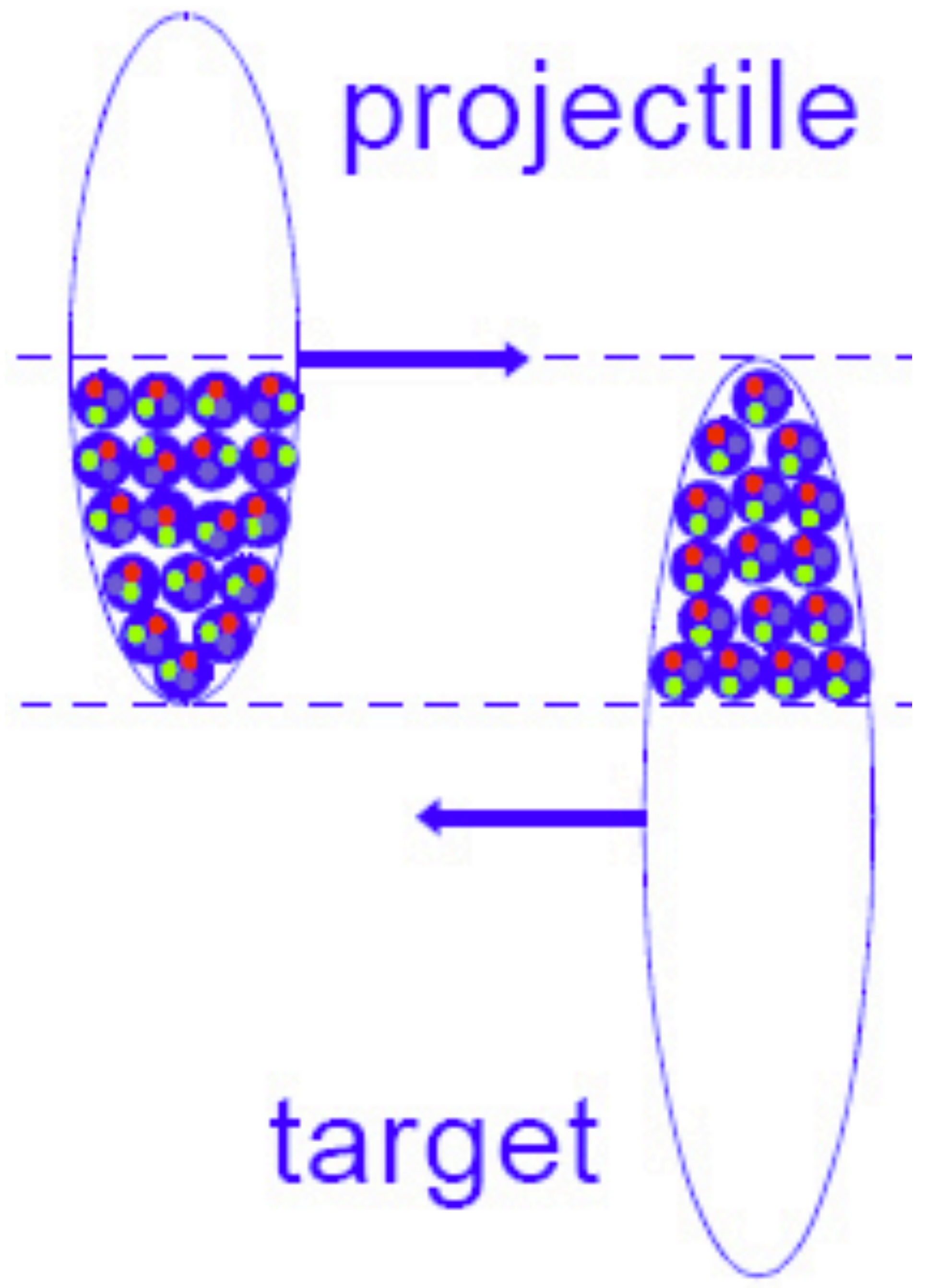

- NEW: rapidity-independent "plateau" component in initial baryon profile & tilted baryon peaks describing the varying baryon stopping in the transverse plane

L. Du, C. Shen, S. Jeon & C. Gale, arXiv:2211.16408

DIRECTED FLOW OF MESONS

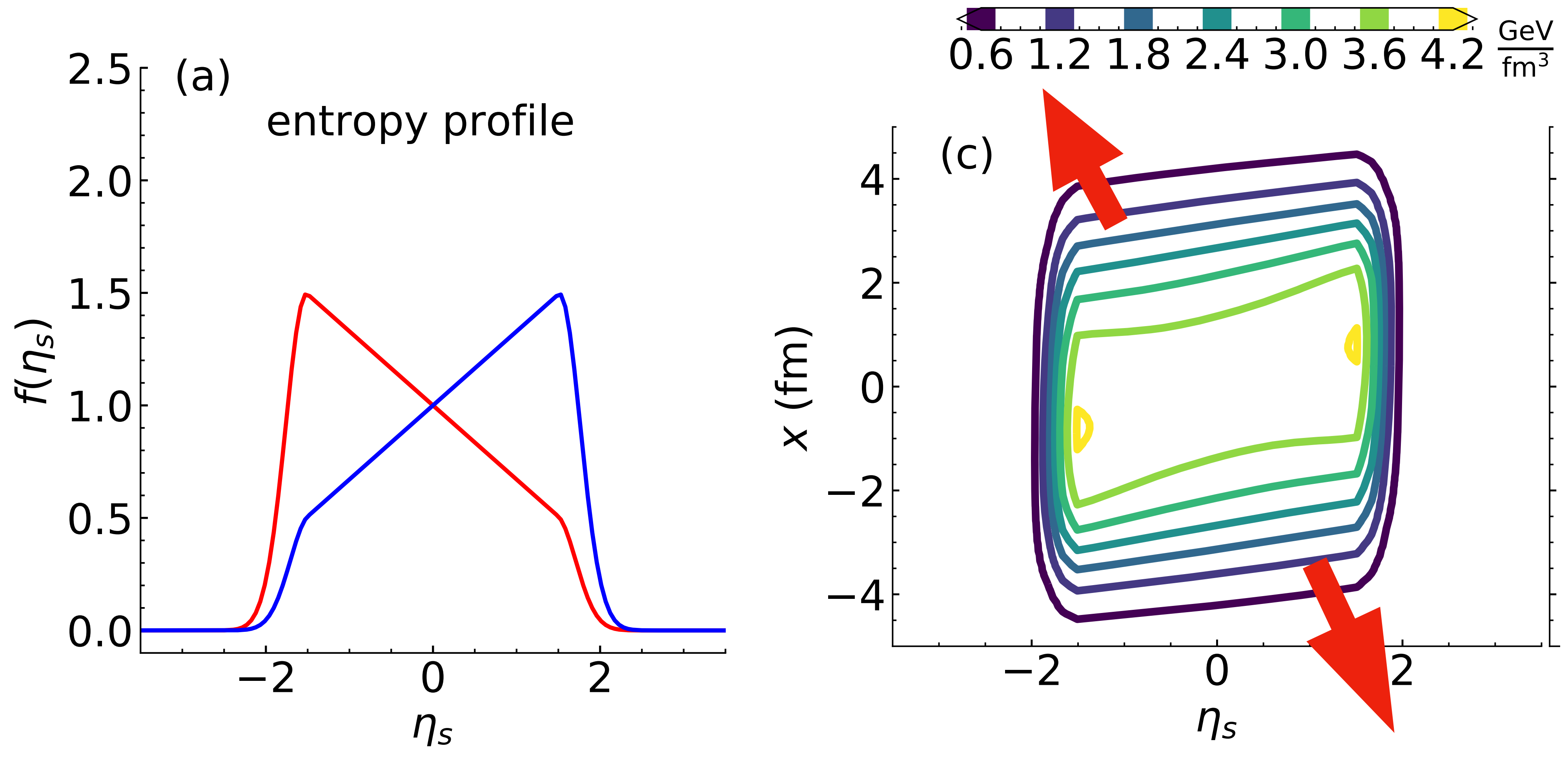

Initial distributions in reaction plane for 10-40%
Au+Au@19.6 GeV

- $v_1(y)$ of mesons with negative slope at all beam energies; slope increases when beam energy decreases
- Slight shift of energy density along x (tilted structure) generates sideward pressure gradient

see also: Bożek & Wyskiel Phys. Rev. C 81, 054902 (2010)

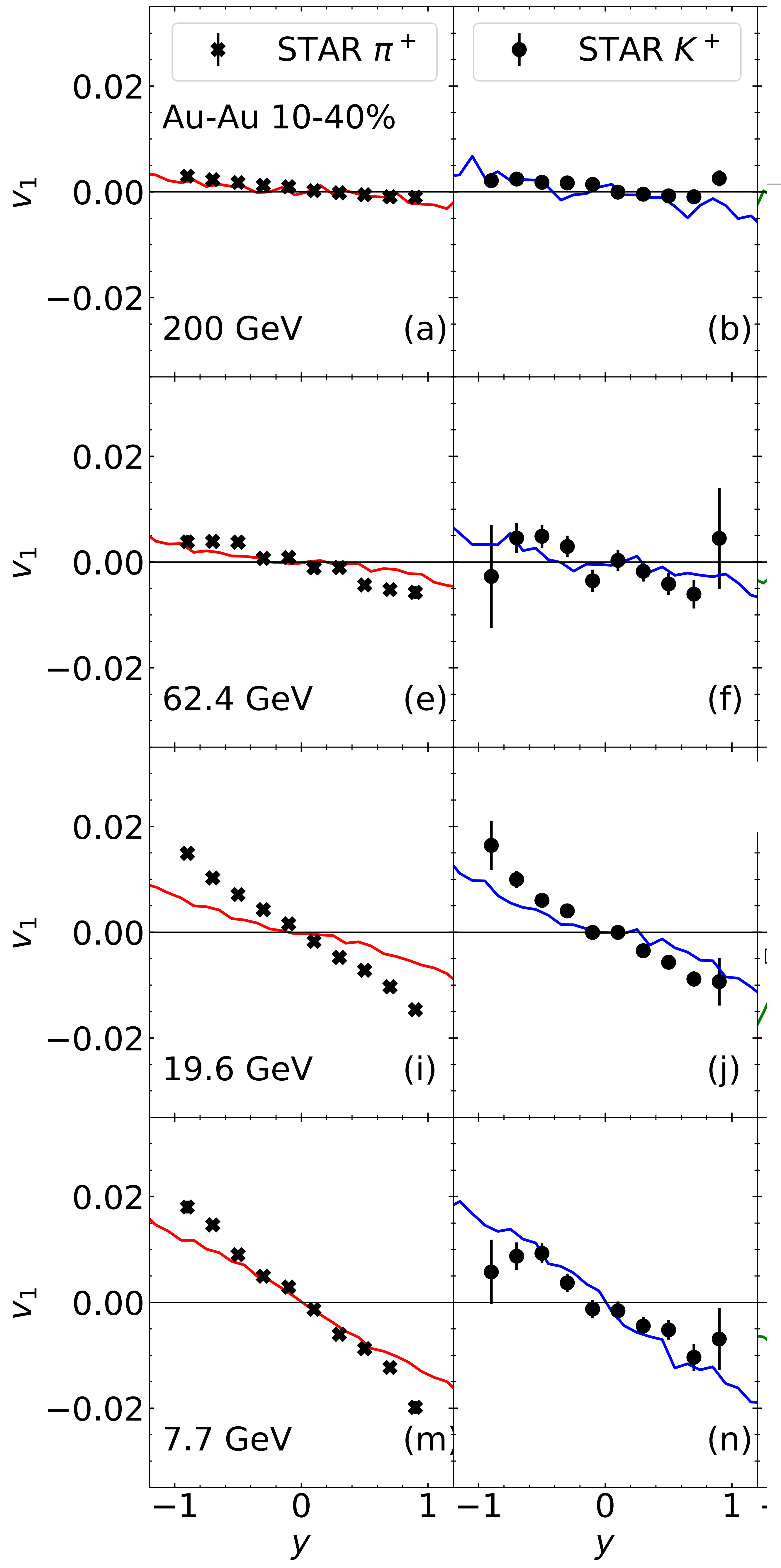

Data: STAR, PRL 112, 162301 (2014); PRL 120, 062301 (2018)

DIRECTED FLOW OF BARYONS

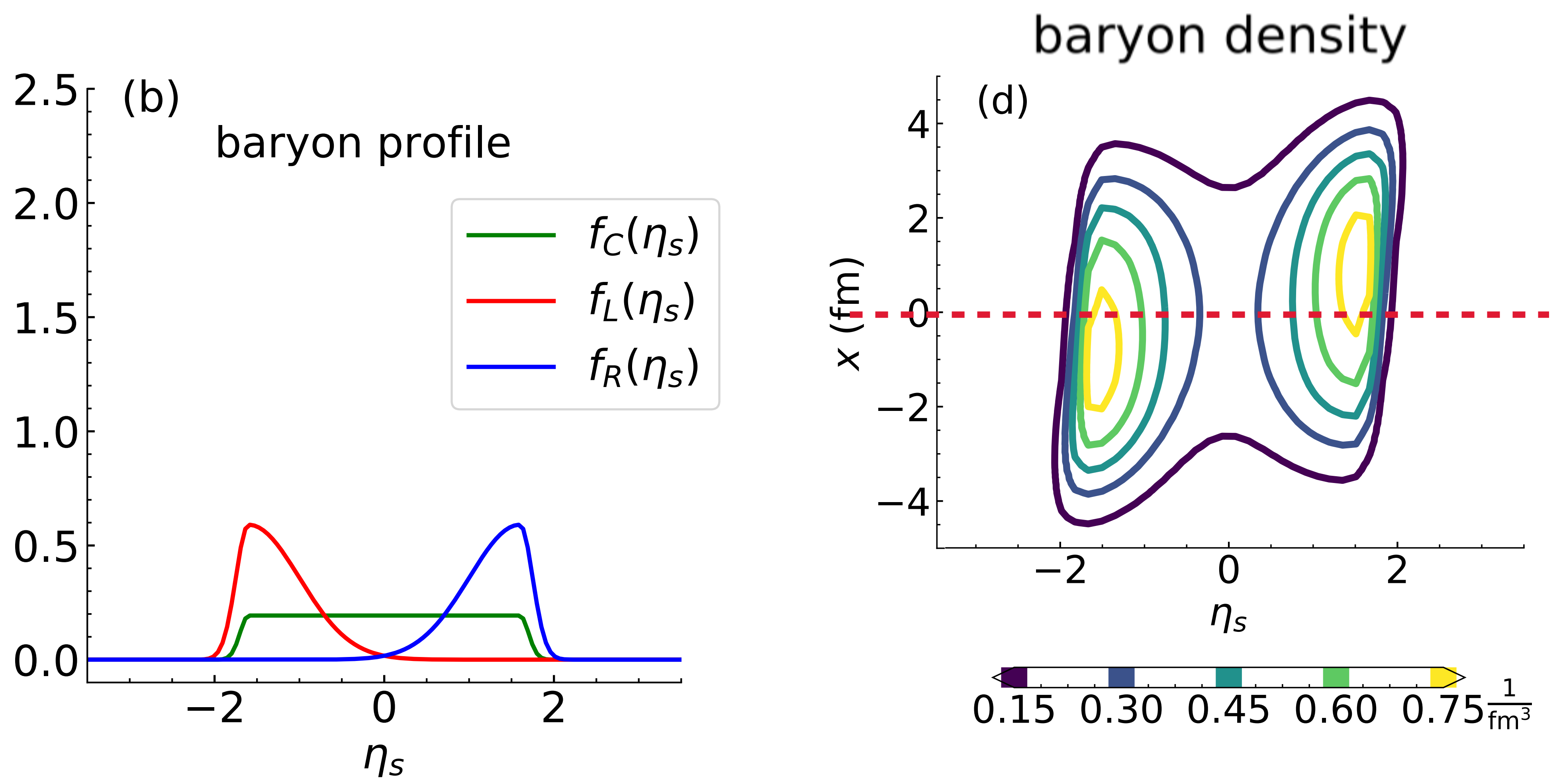

Initial distributions in reaction plane for 10-40% Au+Au@19.6 GeV

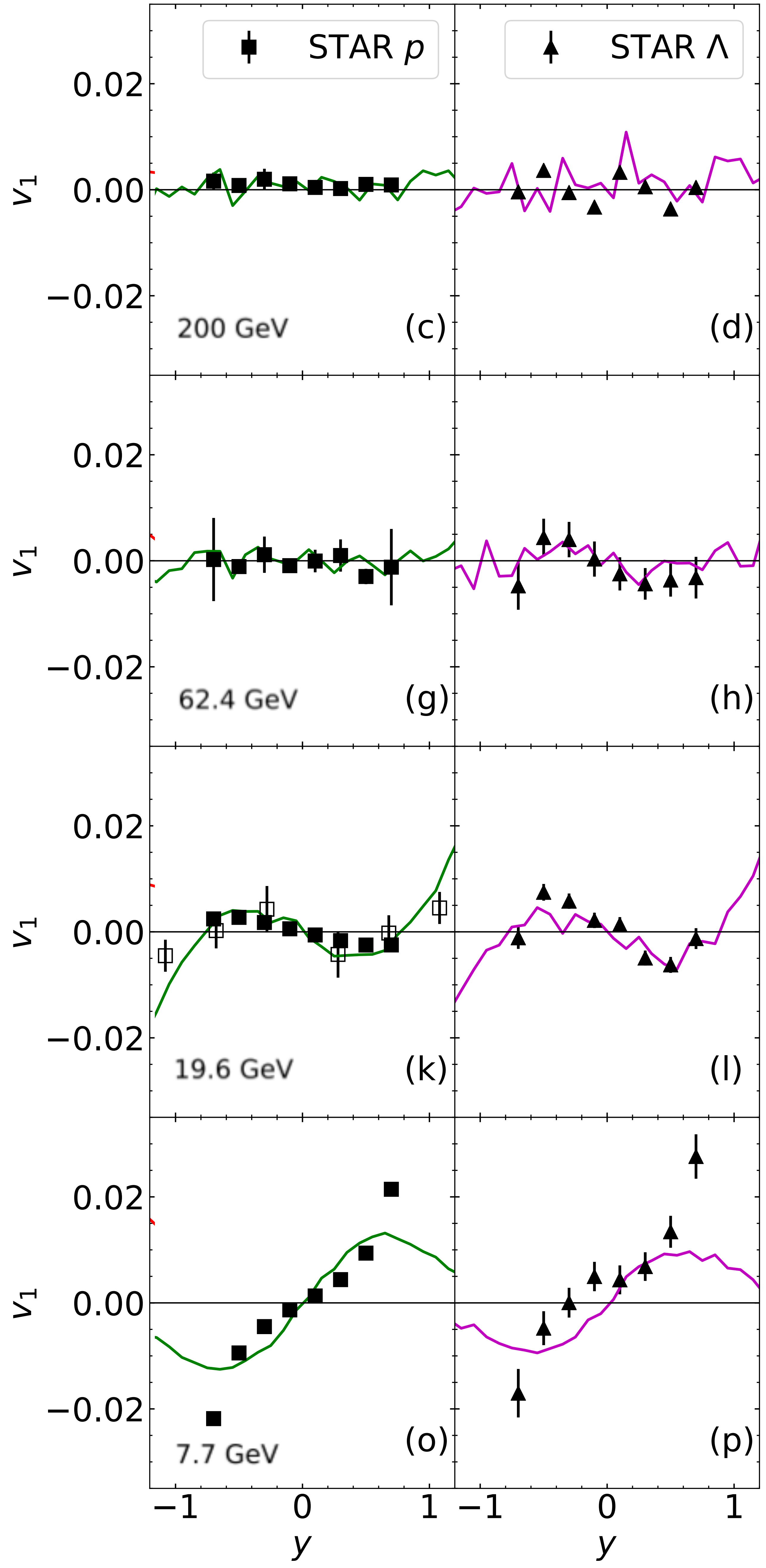

- Nicely reproduce the following features:
  - Flat and small $v_1(y)$ at 62.4 and 200 GeV;
  - cubic rapidity dependent $v_1(y)$ at 19.6 GeV;
  - $v_1(y)$ with positive slope at 7.7 GeV.

Data: STAR, PRL 112, 162301 (2014); PRL 120, 062301 (2018)

DIRECTED FLOW OF BARYONS AT 19.6 AND 7.7 GEV

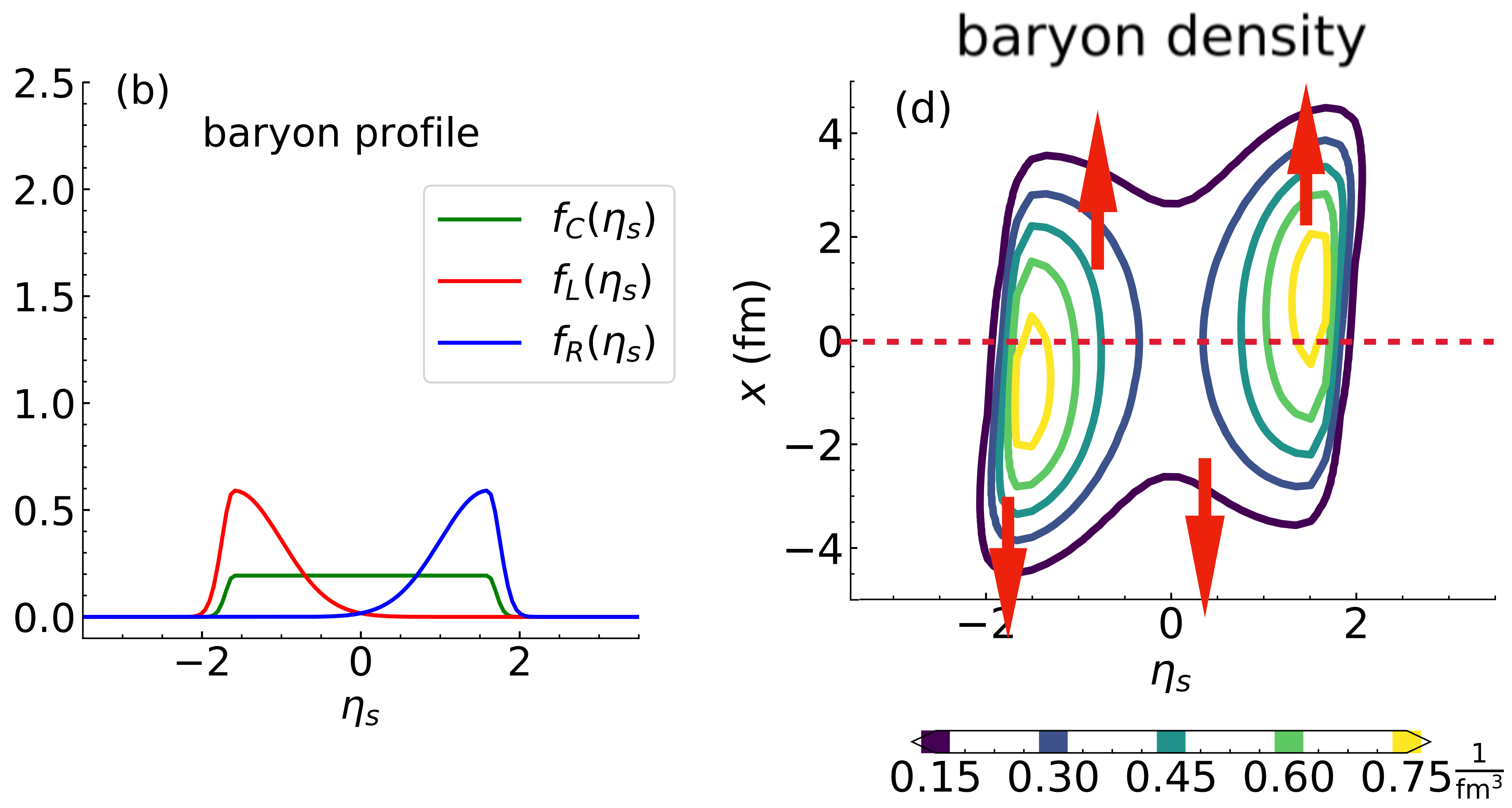

Initial distributions in reaction plane for 10-40% Au+Au@19.6 GeV

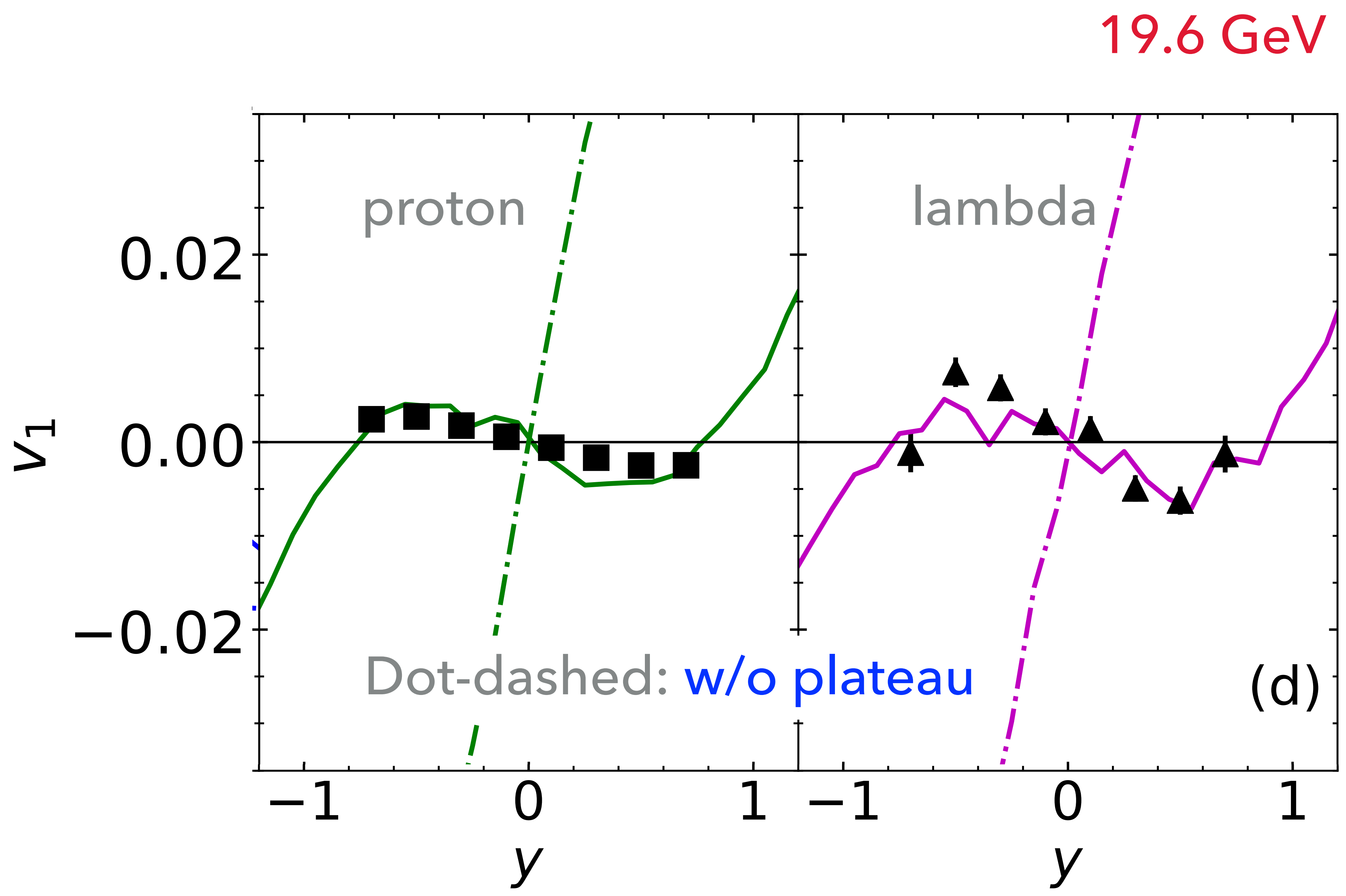

- Initial baryon distribution: central plateau + tilted peaks
- Transverse expansion + asymmetric distribution of baryon density along x ⟹ double sign change in the slope of $v_1(y)$ for baryons at 19.6 GeV, and positive slope at 7.7 GeV

DIRECTED FLOW OF BARYONS AT 19.6 AND 7.7 GEV

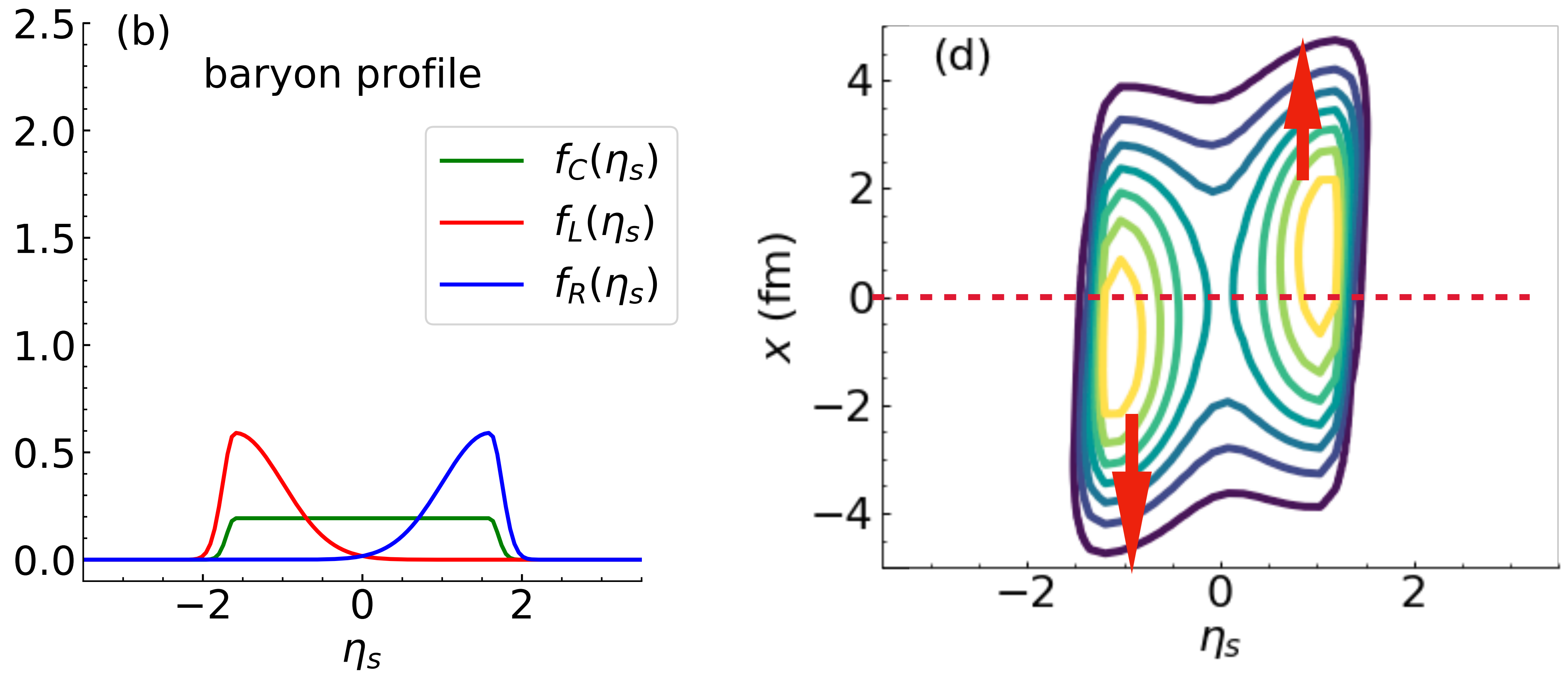

Initial distributions in reaction plane for 10-40% Au+Au@19.6 GeV

7.7 GeV

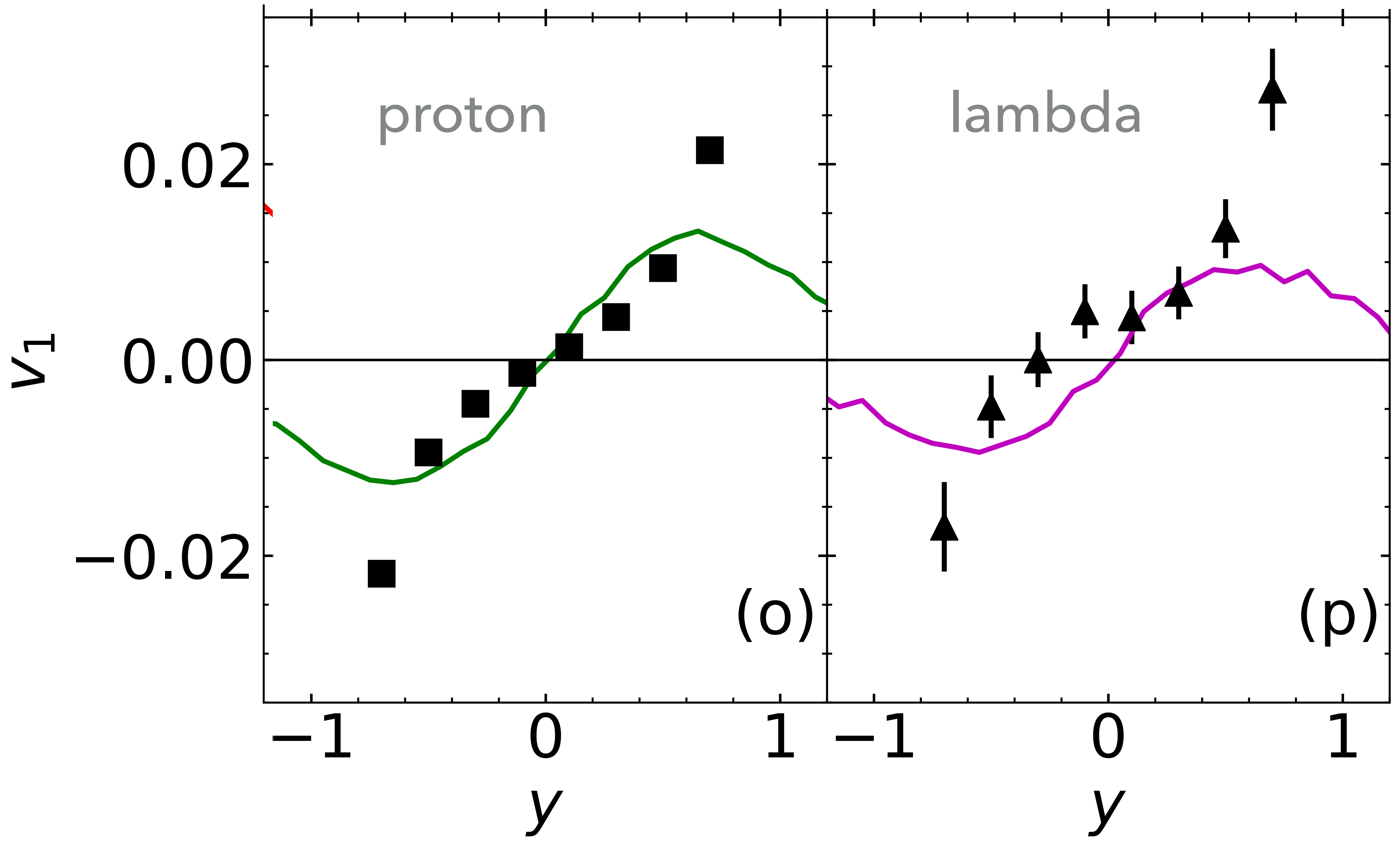

- Initial baryon distribution: central plateau + tilted peaks
- Transverse expansion + asymmetric distribution of baryon density along x $\Longrightarrow$ double sign change in the slope of $v_1(y)$ for baryons at 19.6 GeV, and positive slope at 7.7 GeV

INITIAL BARYON "STOPPING"?

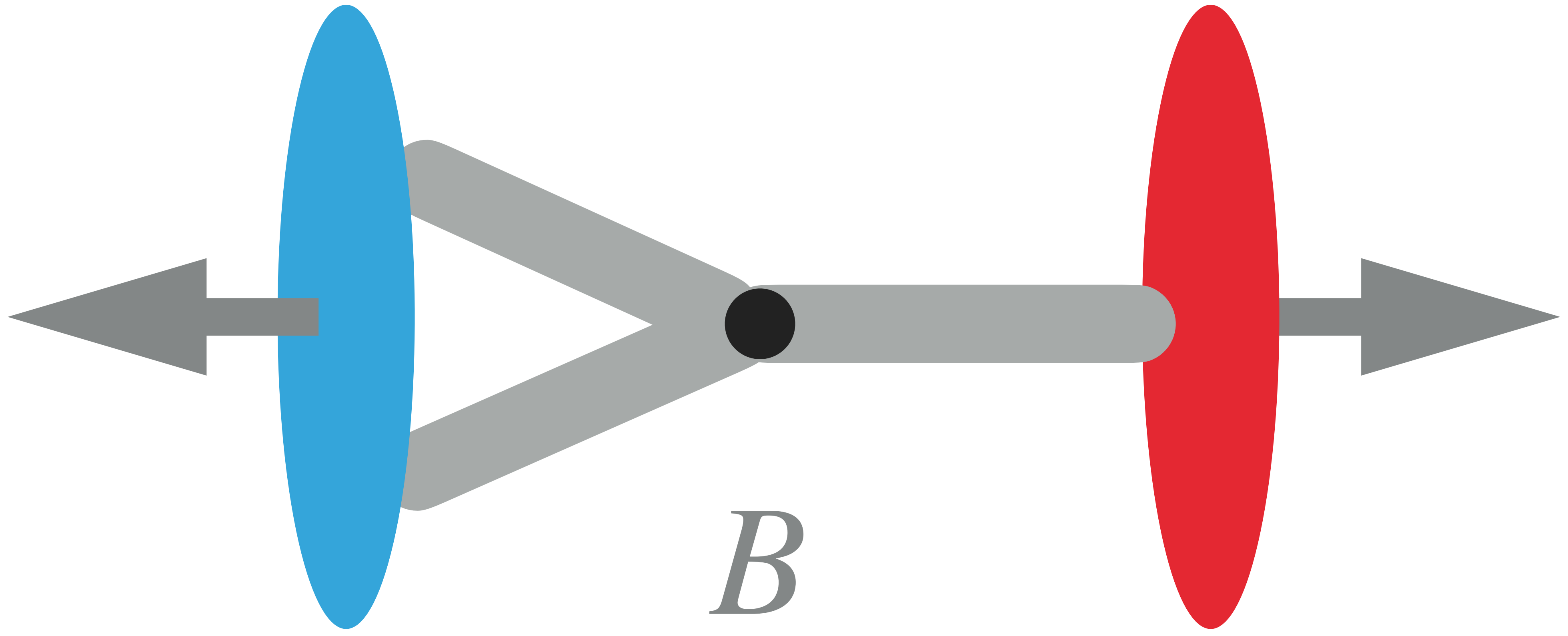

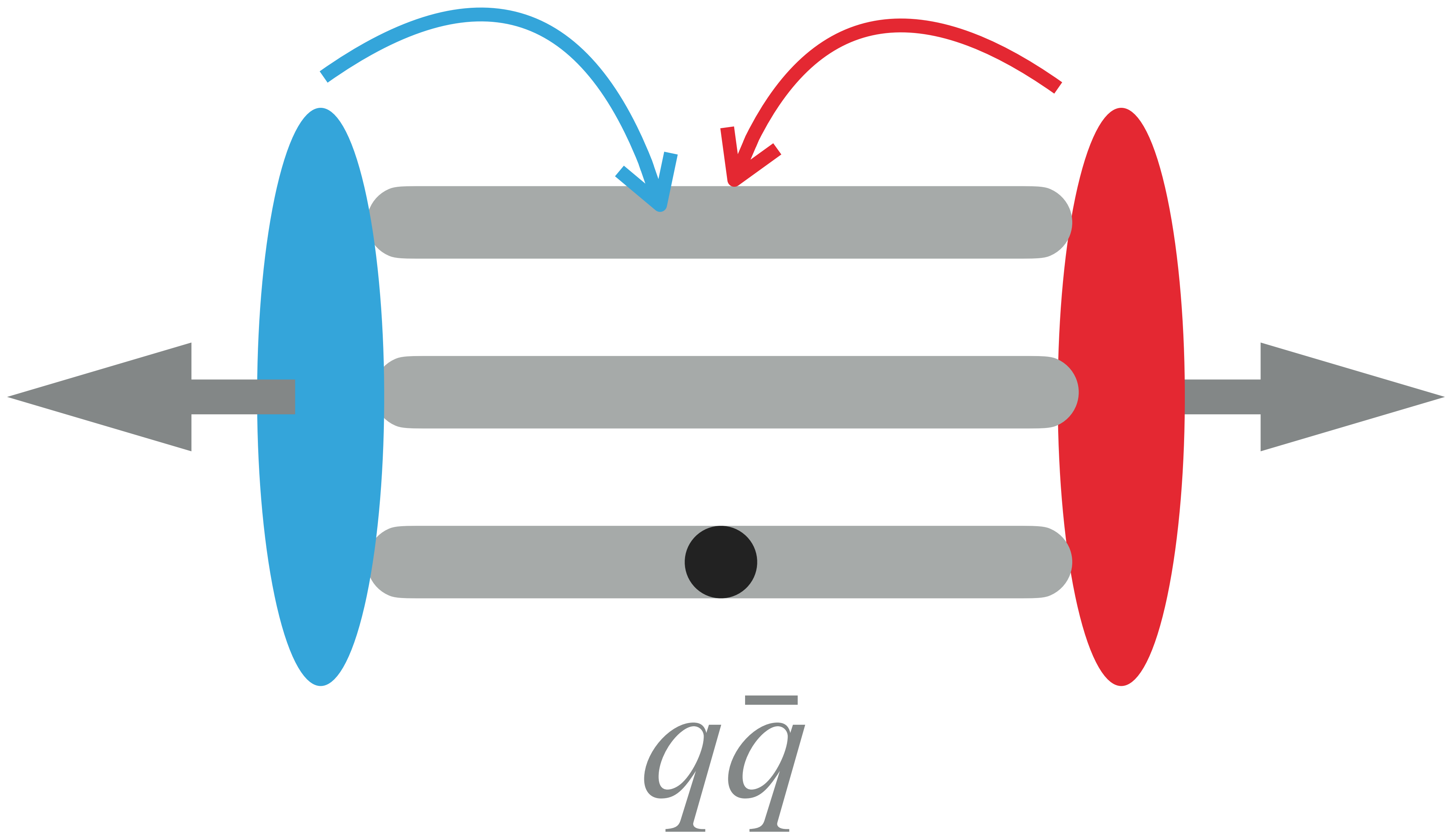

- Right: baryons distributed in rapidity through string junction breaking; less energy loss
- Left: baryon stopped by deceleration of the incoming nucleons; more energy loss

String junction: Kharzeev, PLB 378, 238 (1996)

EXTRACTING FINAL BARYON DISTRIBUTION

FREEZE-OUT DISTRIBUTION @ 19.6 GEV

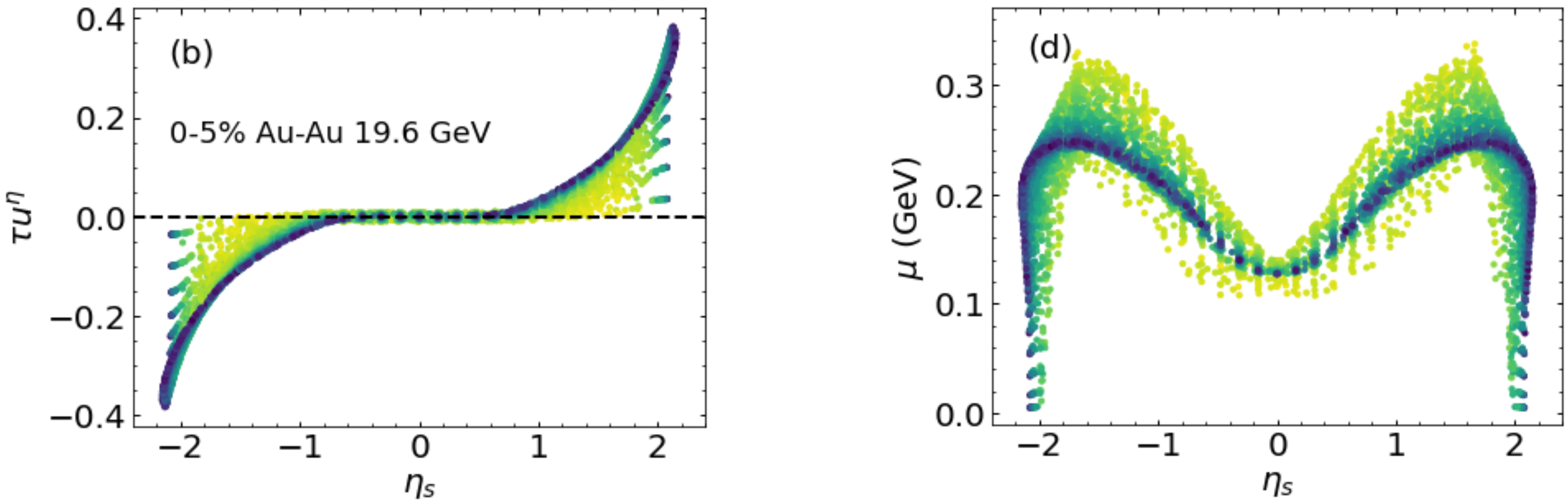

- Strongly broken boost-invariance, especially at forward-/backward rapidities
- Driven by pressure gradients due to longitudinal inhomogeneity
- Large variation in μ_B along rapidity

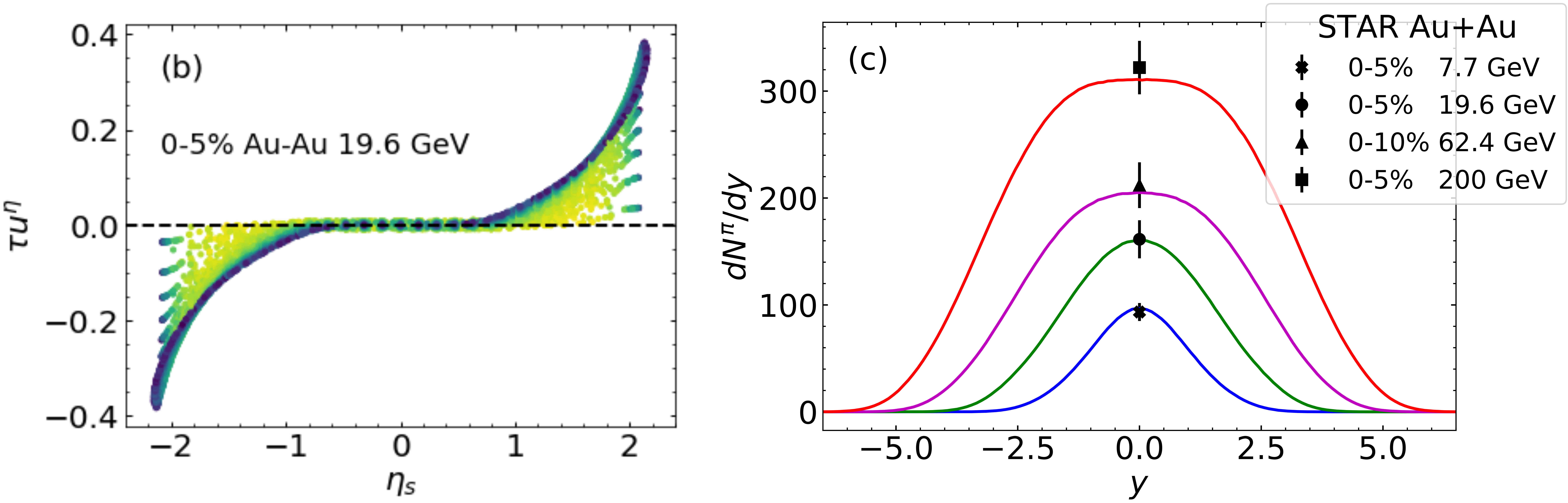

- At 19.6 GeV, the system extends to $|\eta_s| \lesssim 2.5$, but particles reach $|y| \approx 4$
- Two reasons: thermal smearing + longitudinal boost
- Particles produced at forward rapidities may be boosted from a smaller η_s

THERMAL YIELDS AT CHEMICAL FREEZE-OUT

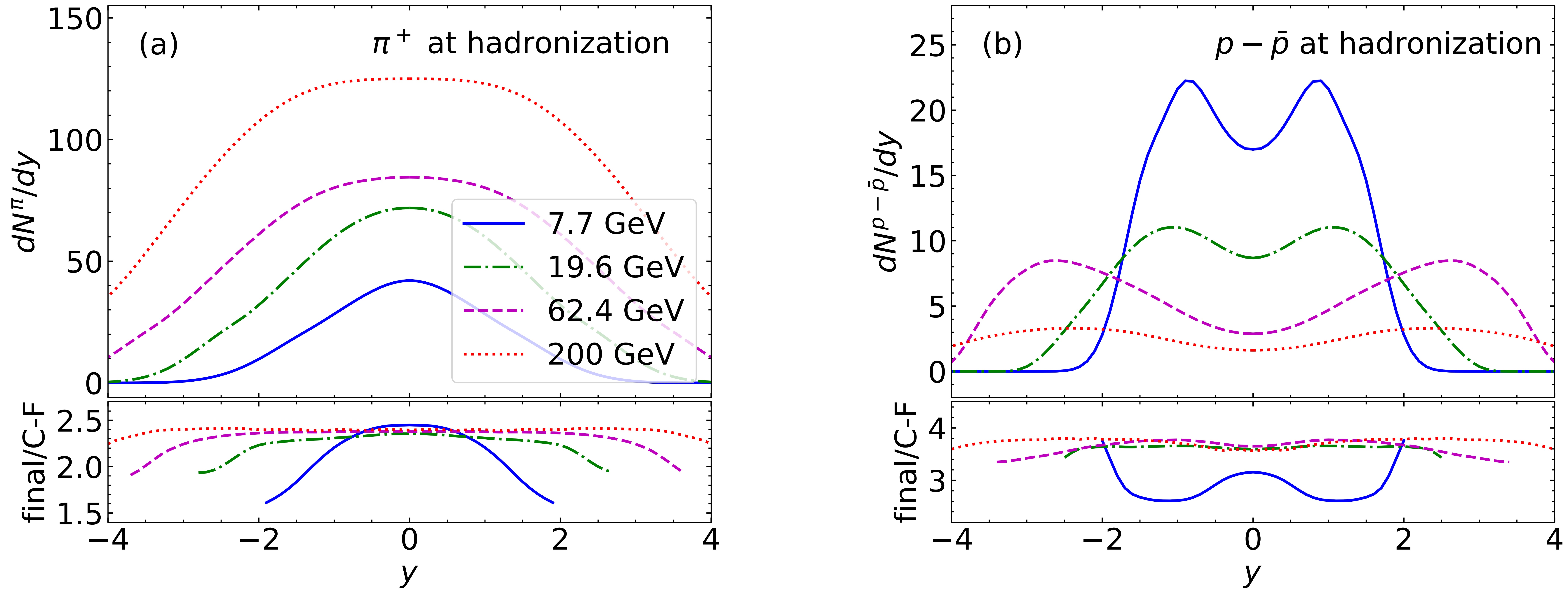

- Identified particle yields change during the afterburner because of resonance decay;
- The ratio between "final" (with decays) and "Cooper-Frye" (thermal) yields can vary along rapidity;
- Correction of the feed-down effect needs to consider rapidity-dependence.

THERMAL YIELDS FROM A STATIC SOURCE

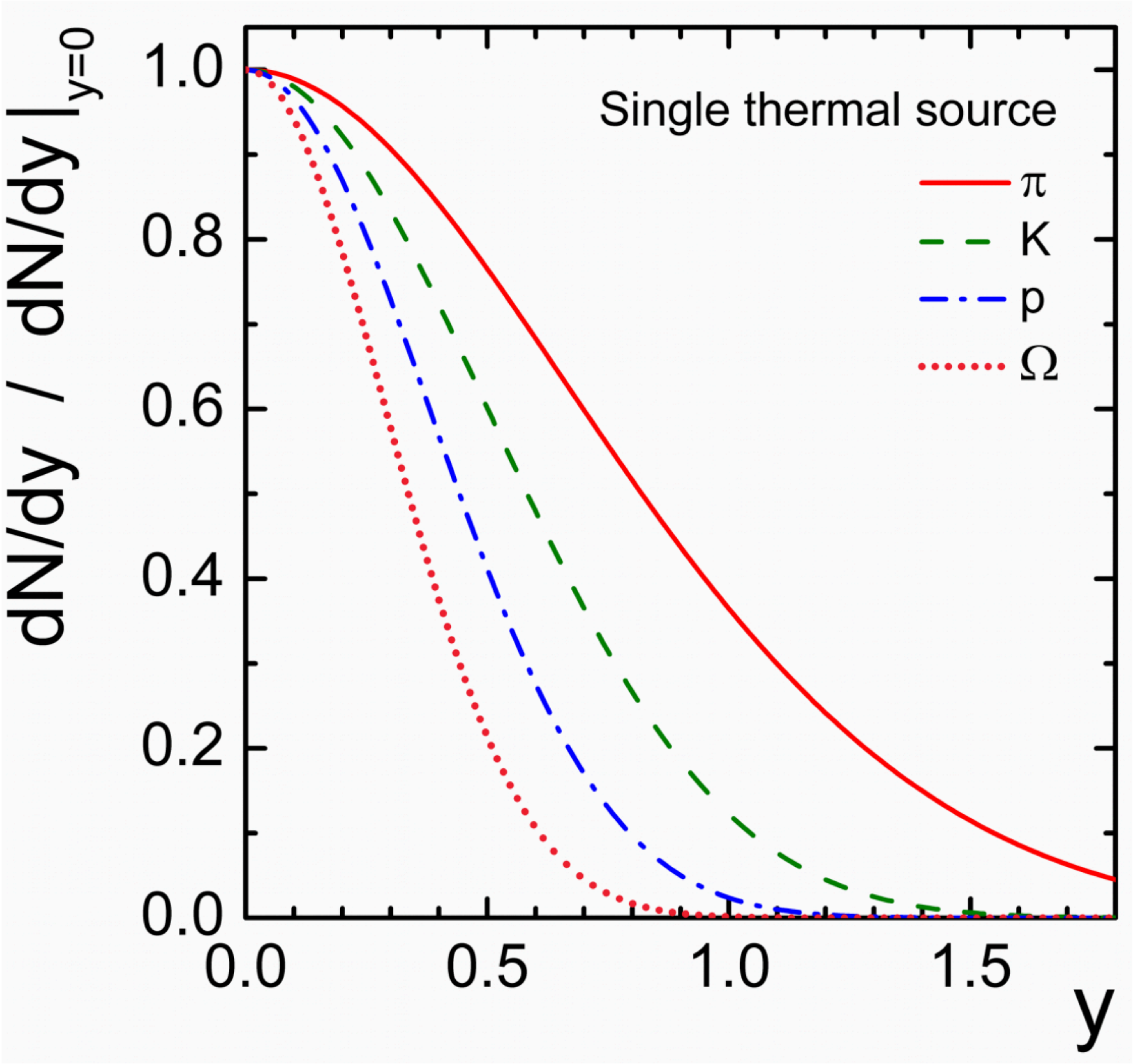

- The rapidity distributions from a static thermal source have a Gaussian-like shape
- The full width at half-maximum:
  - pion: 1.6; kaon: 1.2; proton: 0.9
- Essential to consider thermal smearing for longitudinally inhomogeneous system

V. Begun et al., PRC 98, 034905 (2018)

EXTRACTED FREEZE-OUT PROFILES

- Around mid-rapidity with $|y_s| \lesssim 2$, the two scenarios give similar (T, μ_B);
- Large theoretical uncertainties are observed at forward rapidities;
- Significant uncertainties in the extracted profiles are unavoidable for the discrete model when the yields are small.

LONGITUDINAL BOOST

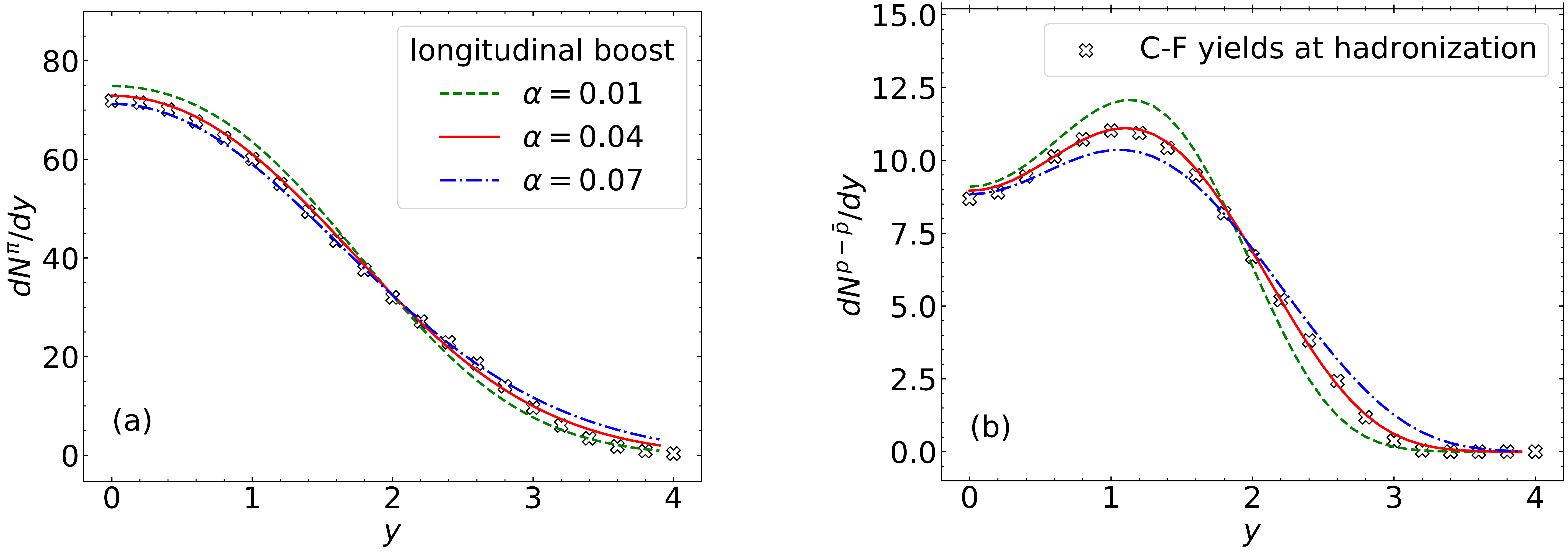

- Starting from the same $T(\eta_s), \mu_B(\eta_s)$ profiles, the distributions get stretched in with a larger longitudinal flow y, which is more strongly for heavier species.

LONGITUDINAL SYSTEM SIZE

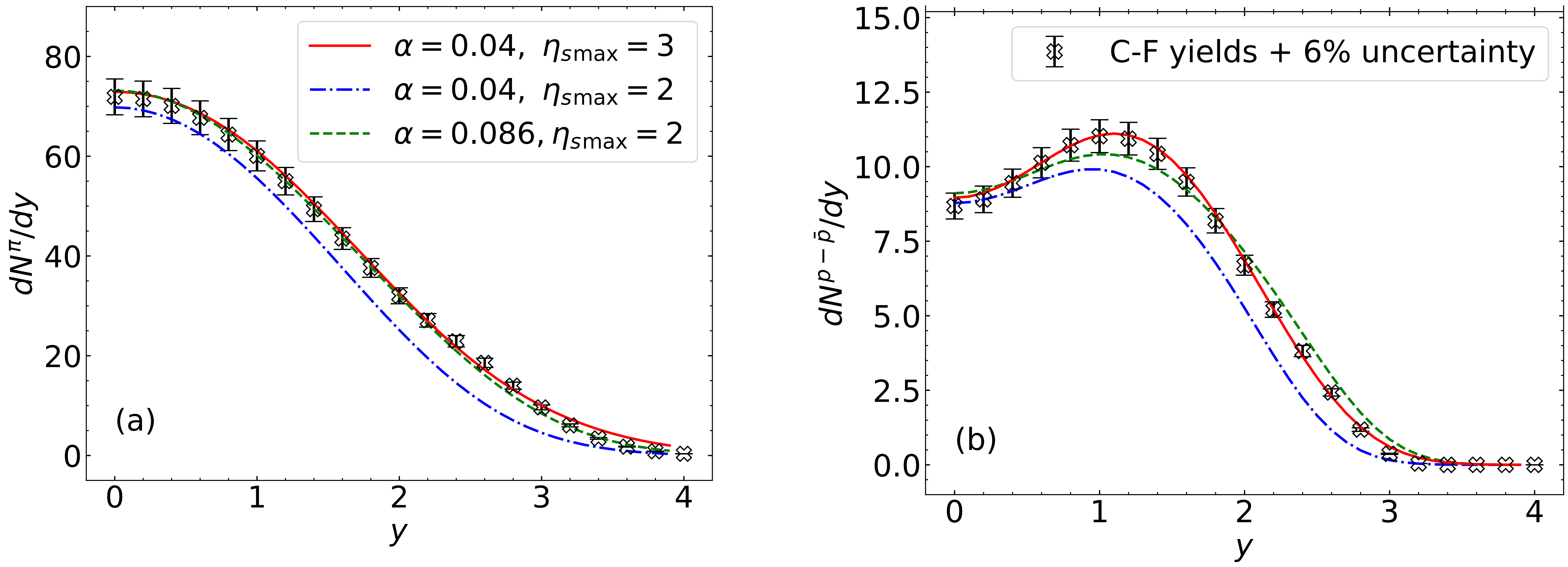

- A smaller system size in η_s can be compensated by a more considerable longitudinal boost and a larger volume.

SUMMARY AND OUTLOOK

SUMMARY AND OUTLOOK

I. Initial baryon distribution

- We introduced a central plateau component in the initial baryon distribution, which is essential for explaining characteristic features of $v_1(y)$ at various beam energies.
- Baryon distributions from deceleration and string junction breaking correspond to different energy loss.

II. Final baryon distribution

- Large rapidity variations in thermodynamic properties are found at low beam energies.
- Longitudinal flow that is faster than Bjorken flow is developed due to longitudinal inhomogeneity.
- Thermal smearing, longitudinal boost, and system size can affect the rapidity-dependent distributions.

THANK YOU!

INITIAL PROFILES AND PARAMETERS

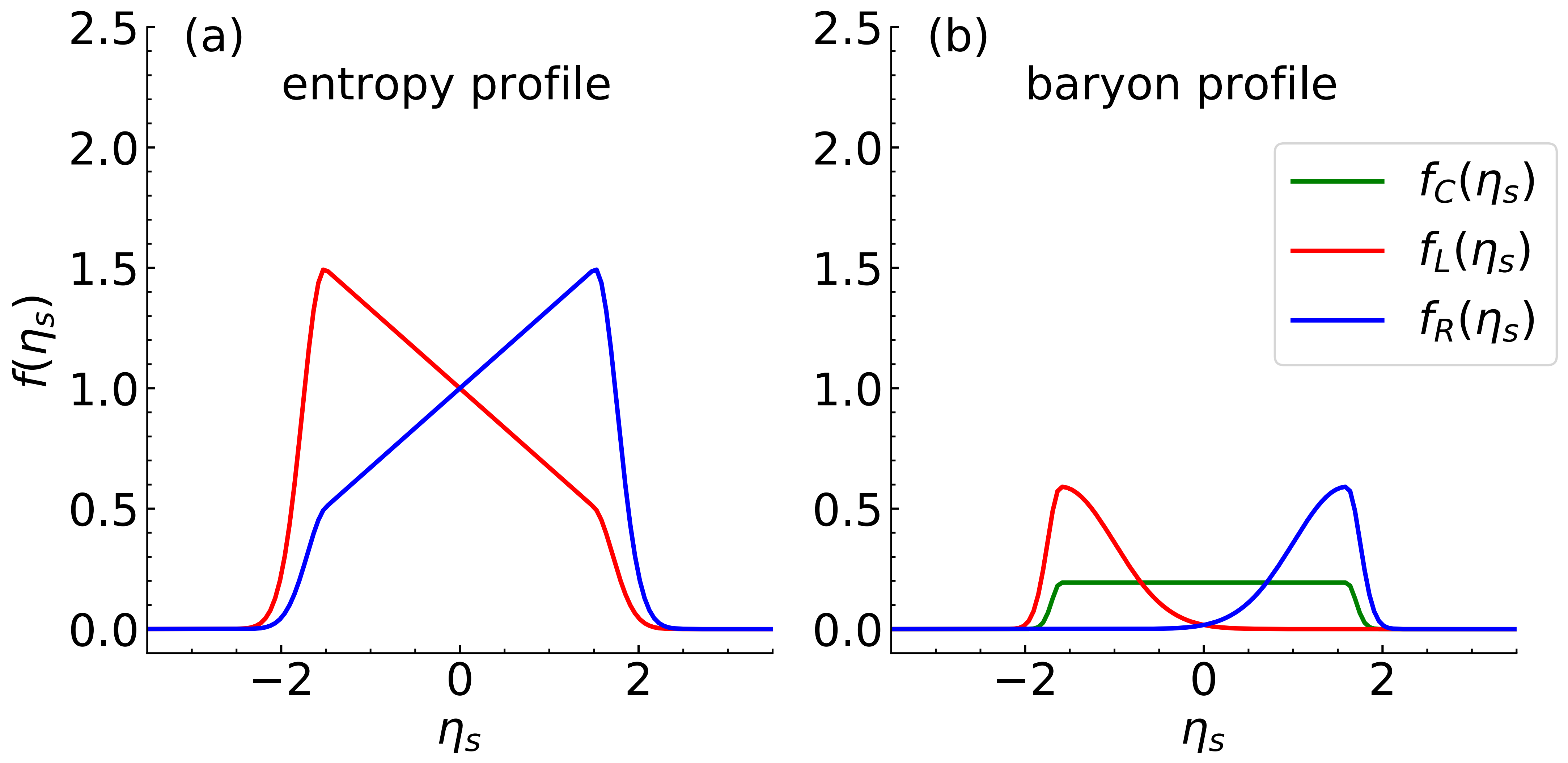

baryon profile

$$n(\tau_0, \boldsymbol{x}_\perp, \eta_s) = \frac{N_B}{\tau_0}\Big\{ f_-^B[\eta_L(\boldsymbol{x}_\perp)]T_- + f_+^B[\eta_L(\boldsymbol{x}_\perp)]T_+ + \cosh^{-2}[r(\boldsymbol{x}_\perp)]N_c f_c^B(\eta_s)\big(T_- + T_+\big)\Big\},$$

$$f_\pm^B(\eta_s) = N\left[\theta(\eta_s - \eta_0^{B,\pm})\exp\left(-\frac{(\eta_s - \eta_0^{B,\pm})^2}{2\sigma_{B,\mp}^2}\right) + \theta(\eta_0^{B,\pm} - \eta_s)\exp\left(-\frac{(\eta_s - \eta_0^{B,\pm})^2}{2\sigma_{B,\mp}^2}\right)\right],$$

$$f_c^B(\eta_s) = N' \exp\left[-\frac{(|\eta_s| - \eta_0^B)^2}{2{\sigma_{\eta,B}}^2}\theta(|\eta_s| - \eta_0^B)\right]$$

$$\eta_L(\boldsymbol{x}_\perp) \equiv [\eta_s - y_L^B y_{\rm cm}(\boldsymbol{x}_\perp)]$$

entropy profile

$$s(\tau_0, \boldsymbol{x}_\perp, \eta_s) = s_0[f_-^s(\eta_s)T_- + f_+^s(\eta_s)T_+],$$

$$f_\pm^s(\eta_s) = \theta(\eta_{\rm max} - |\eta_s|)\left(1 \pm \frac{\eta_s}{\eta_{\rm max}}\right) \times \left[\theta(|\eta_s| - \eta_0^s)\exp\left(-\frac{(|\eta_s| - \eta_0^s)^2}{2\sigma_{\eta,s}^2}\right) + \theta(\eta_0^s - |\eta_s|)\right],$$

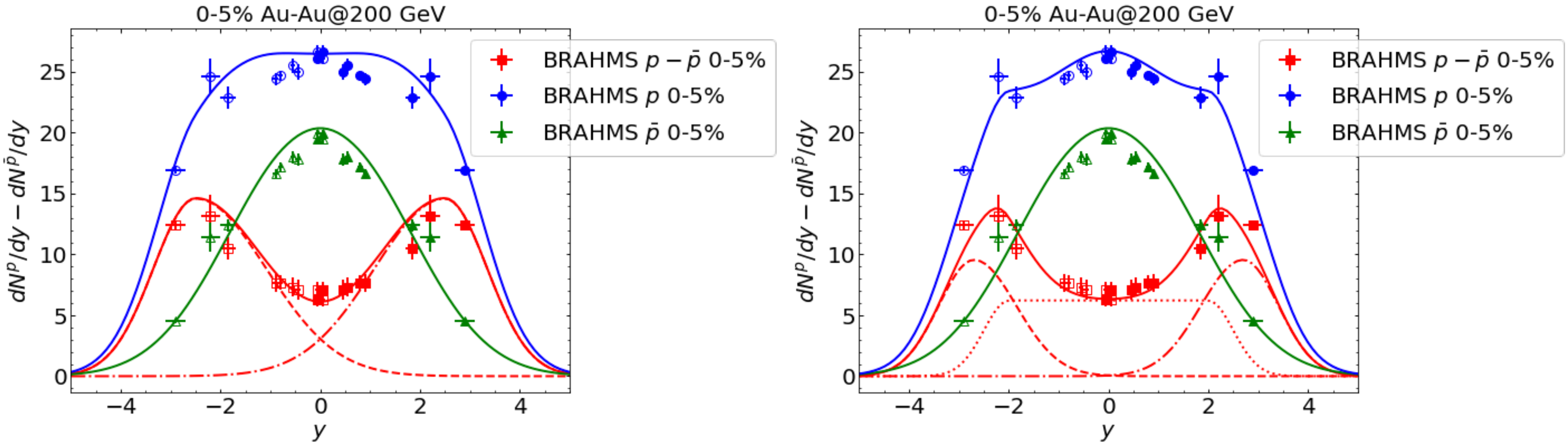

0-5% Au-Au@200 GeV
BRAHMS $p-\bar{p}$ 0-5%
BRAHMS p 0-5%
BRAHMS $\bar{p}$ 0-5%
$dN^p/dy - dN^{\bar{p}}/dy$
y
0-5% Au-Au@200 GeV
BRAHMS $p-\bar{p}$ 0-5%
BRAHMS p 0-5%
BRAHMS $\bar{p}$ 0-5%
$dN^p/dy - dN^{\bar{p}}/dy$
y

TRANSPORT APPROACHES

UrQMD

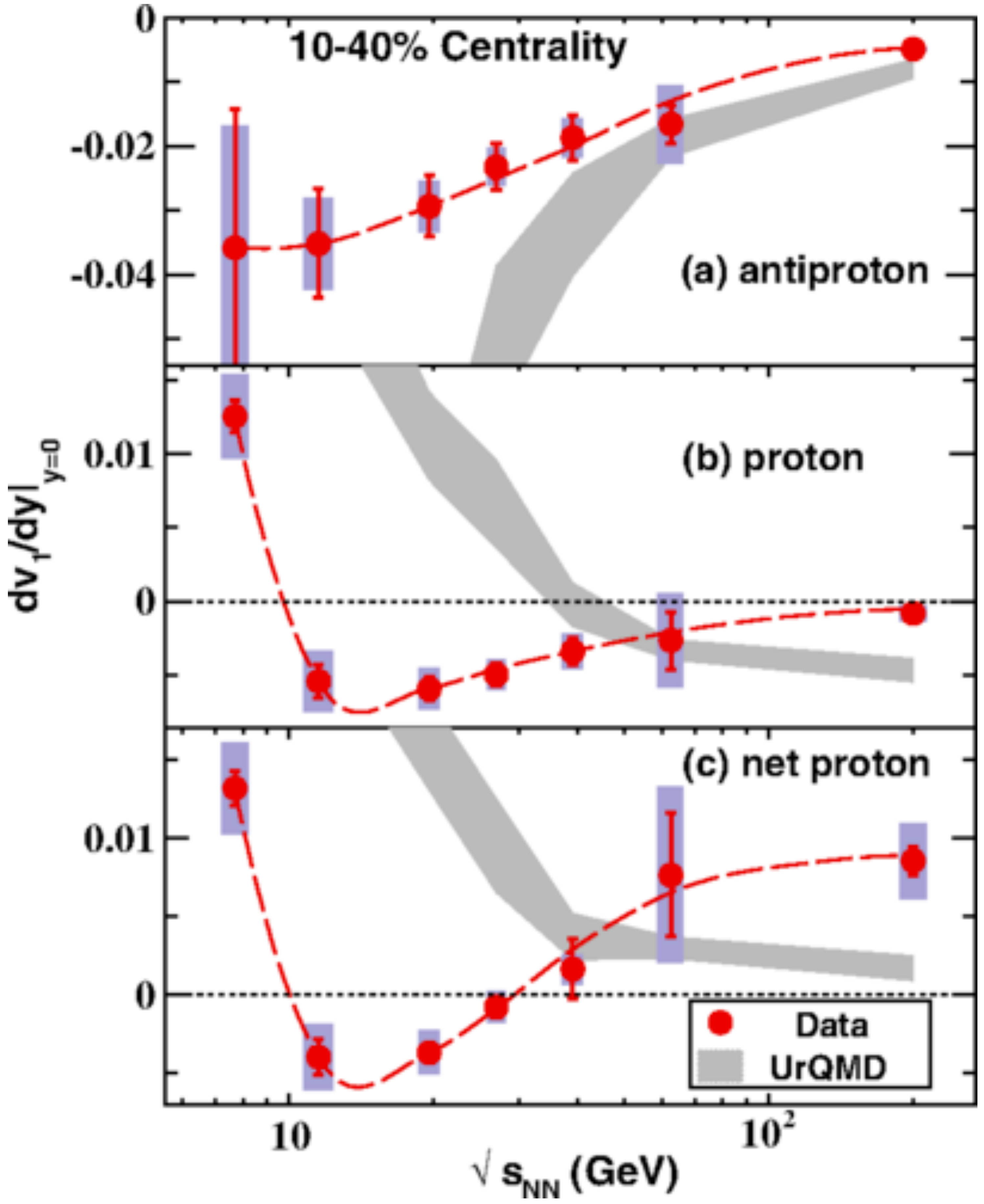

STAR, PRL 112, 162301 (2014)

JAM

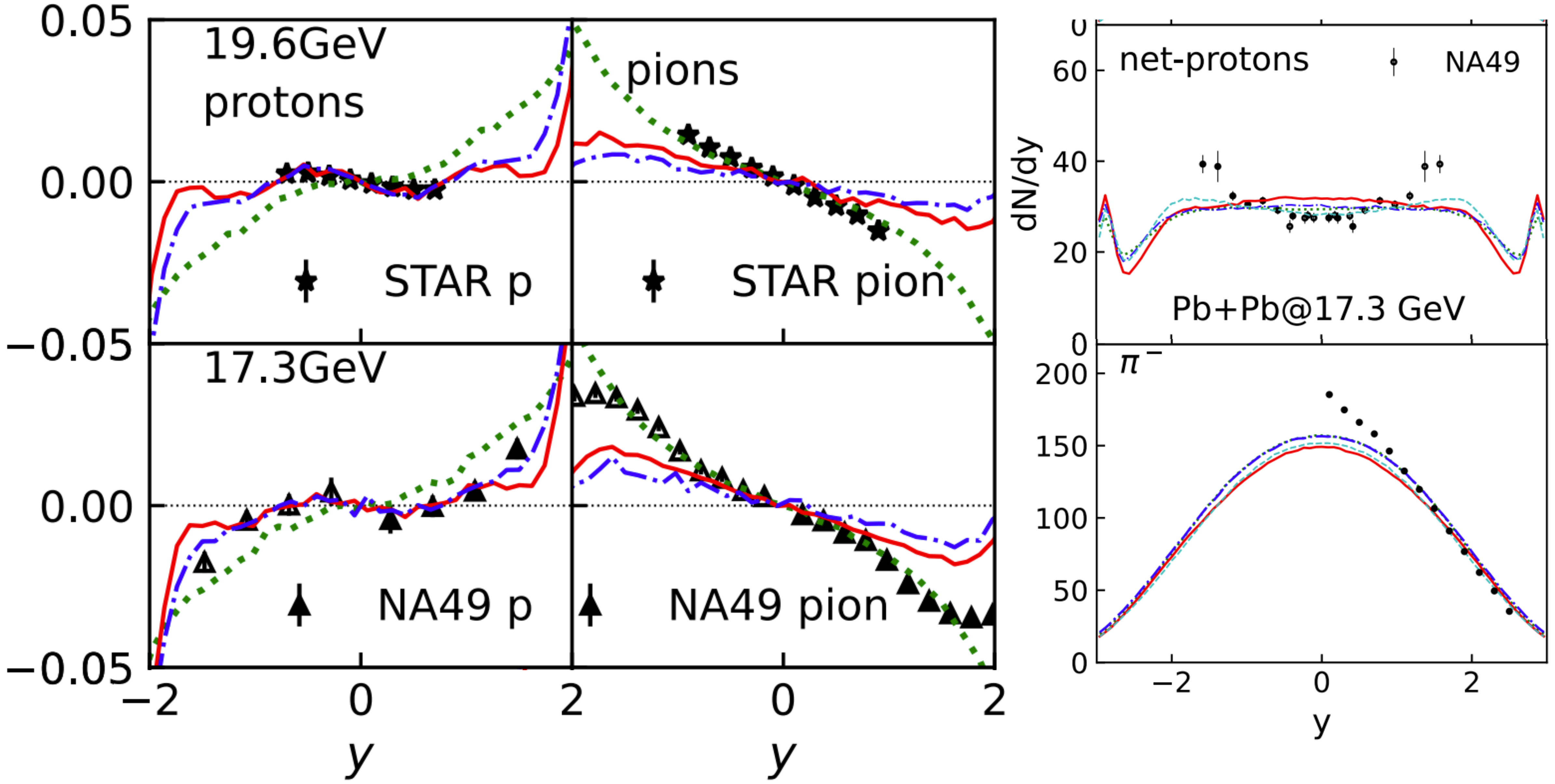

Nara and Ohnishi, PRC 105, 014911 (2022)

FREEZE-OUT DISTRIBUTION @ 19.6 GEV

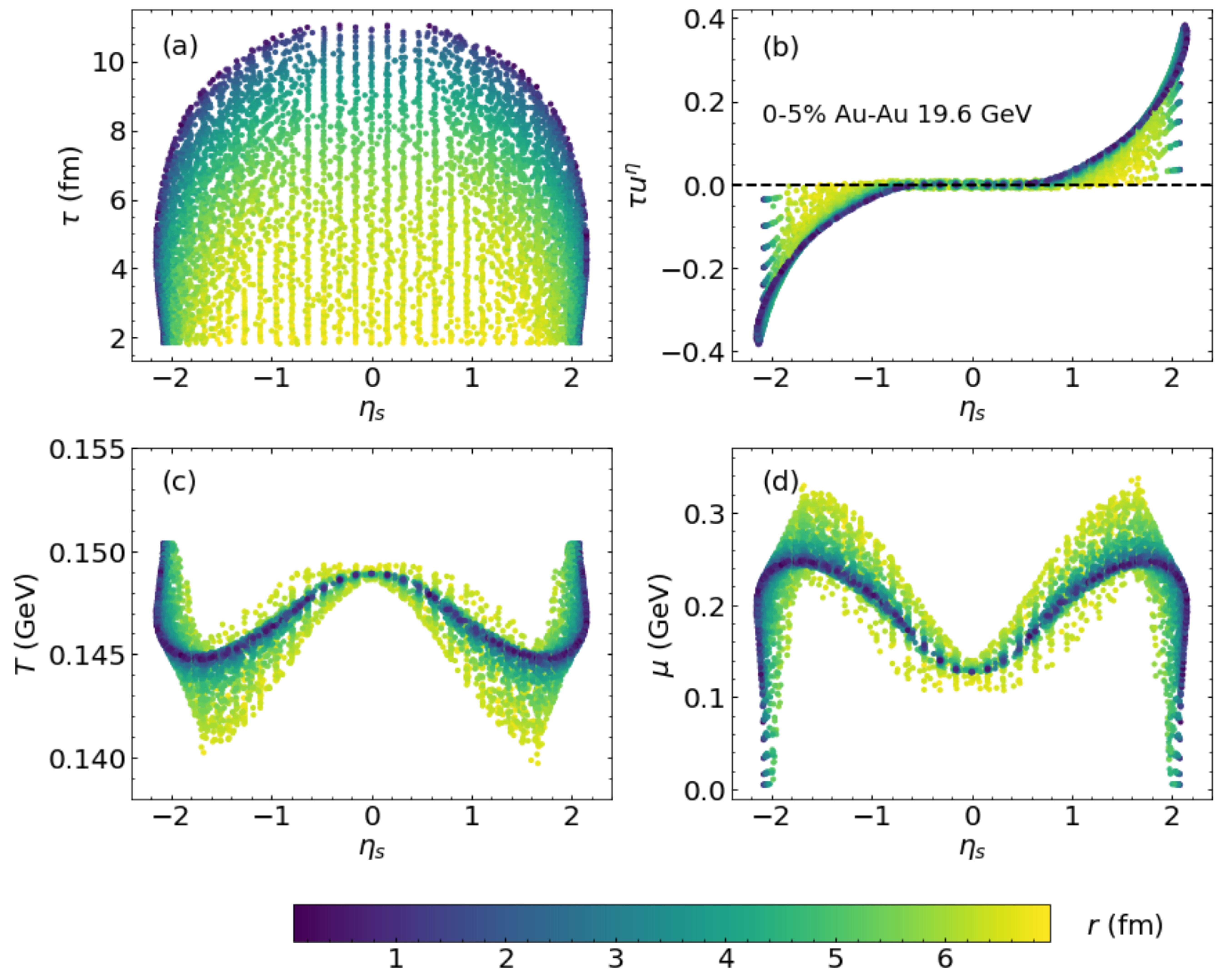

- Strongly broken boost-invariance, especially at forward-/backward rapidities
- Driven by pressure gradients due to longitudinal inhomogeneity
- μ_B and T anti-correlated
- Large variation in μ_B along rapidity

FREEZE-OUT DISTRIBUTION @ BES

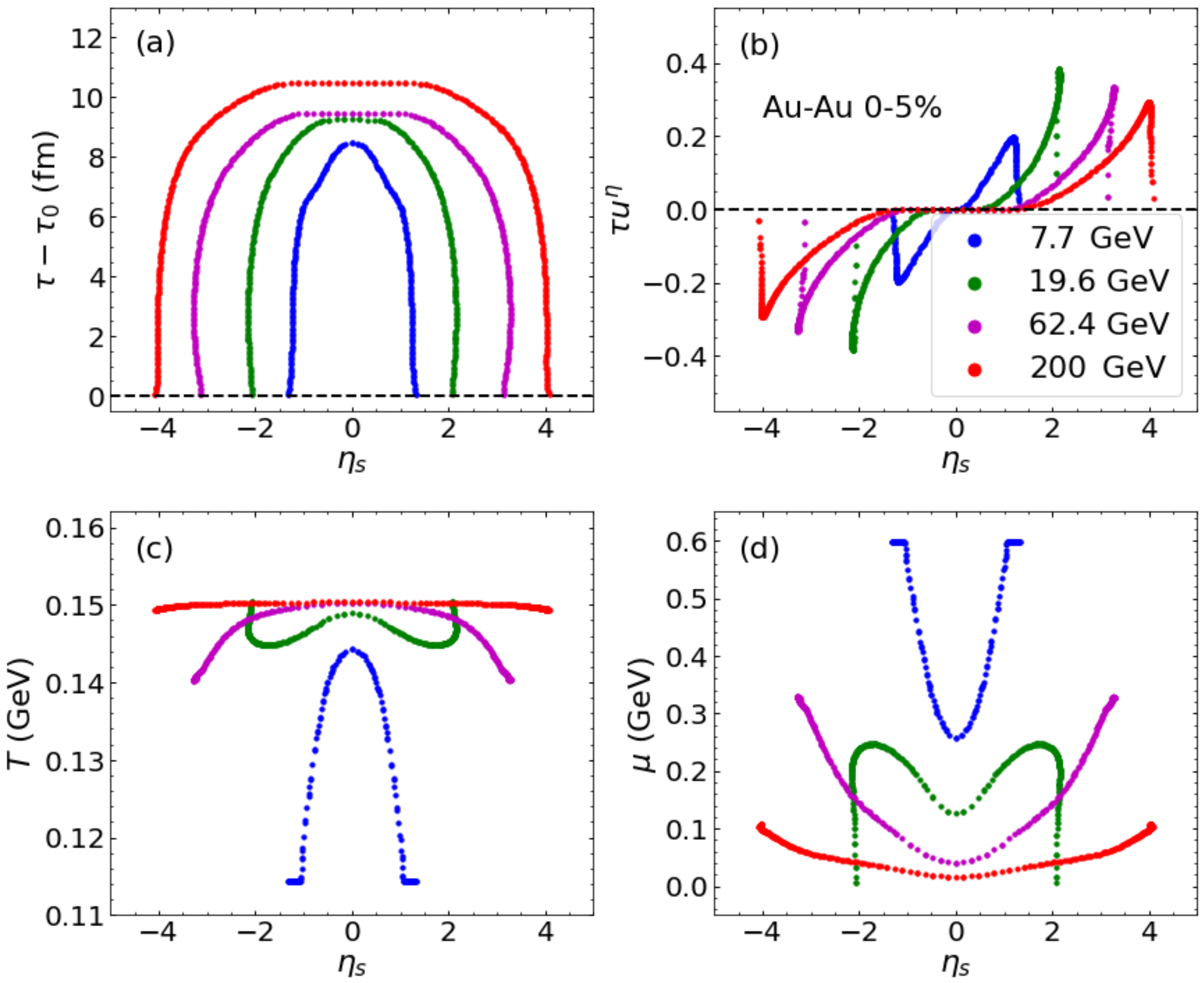

- Boost-invariance is broken more strongly when $\sqrt{s_{\mathrm{NN}}}$ decreases;
- Systems become less isothermal and homogeneous when $\sqrt{s_{\mathrm{NN}}}$ decreases.